

ELECTRONIC ENERGY BAND STRUCTURE OF
COPPER BY TIGHT-BINDING METHOD

By

LIN WANG

Bachelor of Science
National Taiwan University
Taipei, Taiwan
1956

Master of Science
Oklahoma State University
Stillwater, Oklahoma
1966

Submitted to the Faculty of the Graduate College
of the Oklahoma State University
in partial fulfillment of the requirements
for the Degree of
DOCTOR OF PHILOSOPHY
May, 1971

OKLAHOMA
STATE UNIVERSITY
LIBRARY
AUG 12 1970

ELECTRONIC ENERGY BAND STRUCTURE OF
COPPER BY TIGHT-BINDING METHOD

Thesis Approved:

Earl E. Tabor
Thesis Adviser

E. K. Jackson

Leon W. Schwedler

William J. Lewis

E. K. M. Jackson

D. J. Durham
Dean of the Graduate College

788814

ACKNOWLEDGEMENT

The author wishes to take this opportunity to express his gratitude to Dr. E. E. Lafon for suggesting the problem and for his invaluable assistance and guidance in carrying out the research which is to be reported in this thesis.

A special note of thanks goes to Dr. E. E. Kohnke and the members of the Advisory Committee for their encouragement.

It is also a pleasure for the author to express his appreciation to his wife for her constant encouragement.

TABLE OF CONTENTS

Chapter	Page
I. INTRODUCTION	1
A. The Crystal Lattice	3
B. The Wigner-Seitz Unit Cell	4
C. Periodic Functions and Fourier Series	4
D. Atomic Units	7
II. CRYSTAL POTENTIAL	9
A. General Descriptions	9
B. The Coulomb Potential	12
C. The Exchange Potential	21
D. The Fourier Coefficients of Crystal Potential	22
III. GTO TIGHT-BINDING BASIS FUNCTIONS	30
IV. THE SECULAR EQUATION	41
V. CALCULATION OF MULTICENTER INTEGRALS	45
A. Gaussian Orbitals	45
B. Potential Energy Integrals	47
C. Overlap Integrals	60
D. Kinetic Energy Integrals	66
VI. RESULTS AND DISCUSSIONS	74
BIBLIOGRAPHY	81

LIST OF TABLES

Table	Page
I. Curve Fitting Parameters of Charge Density, $\rho_{\text{crys}}^{\text{elec}}(\vec{r})$, and Charge Density to the Third, $[\rho_{\text{crys}}^{\text{elec}}(\vec{r})]^{\frac{1}{3}}$	17
II. Comparison of Tabular and Curve Fit of Charge Density, $\rho_{\text{crys}}^{\text{elec}}(\vec{r})$	18
III. Comparison of Tabular and Curve Fit of Charge Density to the Third, $[\rho_{\text{crys}}^{\text{elec}}(\vec{r})]^{\frac{1}{3}}$	23
IV. Fourier Coefficients of Crystal Potential, $V(\vec{r})$	27
V. Overlap Integrals of the 3d GTO's	35
VI. Curve Fitting Parameters of the 3d Radial Wave Function of Copper	38
VII. Comparison of Tabular and Curve Fit of the 3d Radial Wave Function of Copper.	39
VIII. Analytical Expressions of the Potential Energy Integrals.	61
IX. Analytical Expressions of the Kinetic Energy Integrals. .	70
X. $E(\vec{k})$ Vs. \vec{k} Along [1,0,0] Line in the Brillouin Zone . . .	75
XI. Comparison of the Results From Various Band Structure Calculations of Copper.	76

LIST OF FIGURES

Figure	Page
1. Wigner-Seitz Cell of the Face-Centered Cubic Lattice and the Fundamental Wedge.	5
2. Brillouin Zone of the Face-Centered Cubic Lattice.	8
3. Relations Between Various Vectors Used in the Reduction of the Gaussian Integrals	49
4. $E(\vec{k})$ Vs. \vec{k} Curve Along $[1,0,0]$ Line in the Brillouin Zone. .	78

CHAPTER I

INTRODUCTION

It is the purpose of this investigation to calculate the electronic energy band structure of copper using the tight-binding method with Gaussian-type orbitals (GTO's) as basis functions, and to examine the feasibility of employing this method to calculate energy band structures for other transition metals. A number of energy band calculations of copper with various methods have been reported. Calculations done with cellular method^(1,2) were first reported in 1935, and the latest calculation carried out with the psuedo-potential method⁽³⁾ is reported early last year. During past years, calculations have also been carried out using other methods. They include the orthogonalized plane wave⁽⁴⁾ (OPW), the augmented plane wave^(5,6,7) (APW), the Green's function⁽⁸⁾, and the modified orthogonalized plane wave (MOPW) method⁽⁹⁾.

In most of the above mentioned works, references (1), (2) and (5) through (8), the crystal potential used in the calculations are of the muffin-tin form⁽¹⁰⁾. Indeed the only non muffin-tin attempt to treat the d-bands of copper has been the empirical adaption of psuedo-potential method, and no first principle treatments exist. Reference (4) represents a 1956 attempt at solution using the OPW method and does not attempt to treat the 3d band. Indeed the method of OPW is generally considered to be inapplicable to copper because of its inability to deal with the important d-bands.

The motivation to use the tight-binding method in this investigation is that in this approach one is not limited by the choice of the forms of the crystal potential one may use. Also the tight-binding method yields a more direct and explicit interpretation of energy band formation in solids in terms of atomic orbitals than any of the other methods. Up to this time, no energy band structure calculation for copper by tight-binding method has been reported. In the past, the tight-binding method has generally been regarded as only useful for an approximation^(11,12) to a more complex and detailed band structure calculation, or as an interpolation scheme⁽¹³⁾ to supplement a more detailed calculation. However, this situation has been drastically changed after Lafon and Lin⁽¹⁴⁾ published their work on an energy band calculation of lithium by the tight-binding method in 1966. Their work clearly points out that the tight-binding method can be a quantitative and accurate method when properly applied to an energy band structure problem. At present the tight-binding method is considered as one of the powerful methods to treat energy band problems. Recently, a number of energy band calculations using tight-binding method have been carried out for a few transition metal compounds^(15,17). A recent paper⁽¹⁸⁾ delivered by J. Callaway at an Energy Band Theory Conference held at Watson Laboratory of IBM in New York also seems to help confirm the idea that the tight-binding approach can be a powerful and efficient method for obtaining quantitative results in energy band calculations from the first principle for a variety of materials.

The crystalline copper structure is face-centered cubic (fcc) with a fundamental lattice constant, $a_0 = 3.6147 \text{ \AA} (= 6.8308 \text{ a.u.})$. The crystalline structure of copper can be visualized by recognizing that

there is an atom at each corner of a cube of side, a_0 , and also an atom at the center of each face of the cube. In such a fcc structure, each atom has twelve nearest neighbors. The crystalline solid copper is built upon the repetitions of such cubes. The terminologies needed in treating such periodic structures are given in the following sections.

A. The Crystal Lattice

To describe the crystalline structure of solids one needs a set of three non-coplanar basis vectors, \vec{a}_1 , \vec{a}_2 , and \vec{a}_3 , called basic primitive lattice translation vectors, so defined that a parallelepiped formed by the three primitive vectors is the smallest unit which will build up the lattice by periodic repetition and that the crystalline structure remains invariant under a translation through any vector formed by

$$\vec{R}_n = n_1 \vec{a}_1 + n_2 \vec{a}_2 + n_3 \vec{a}_3 \quad (1-1)$$

where n_1 , n_2 and n_3 are any integers. All points that can be reached by \vec{R}_n are called lattice sites. The lattice sites are merely a set of mathematical points. One only has a crystal by associating an atom or a complex of atoms with each lattice site in the crystal. The parallelepiped defined by \vec{a}_1 , \vec{a}_2 , and \vec{a}_3 having a volume given by $|\vec{a}_1 \cdot (\vec{a}_2 \times \vec{a}_3)|$ is called the primitive unit cell.

From the above considerations, it can be seen that any periodic function $f(\vec{r})$ with the same periodicity as the crystal structure is uniquely defined by the basic primitive vectors \vec{a}_1 , \vec{a}_2 , \vec{a}_3 and by specifying the value of the function at every point in the primitive unit cell.

B. The Wigner-Seitz Unit Cell

The primitive unit cell mentioned in the last section does not clearly show all the possible symmetries that can be associated with the crystal structure. A more convenient alternative choice for the unit cell is the so-called Wigner-Seitz unit cell. The Wigner-Seitz cell has the advantage of displaying the possible rotational symmetry of the crystal more clearly than does the primitive unit cell defined by \vec{a}_1 , \vec{a}_2 and \vec{a}_3 described in Section A. The Wigner-Seitz cell is constructed by setting up planes which are perpendicular bisectors of the vectors from an arbitrarily chosen lattice point to all surrounding lattice sites. The smallest volume enclosed by these planes, and including the origin, i.e., the arbitrarily chosen lattice point, is called the Wigner-Seitz unit cell. The Wigner-Seitz cell for fcc structure is shown in Figure 1.

C. Periodic Function and Fourier Series

A function $f(\vec{r})$ having the same periodicity as the crystal structure must satisfy the following relation

$$f(\vec{r} + \vec{R}_n) = f(\vec{r}) \quad (1-2)$$

where \vec{R}_n is any translation vector defined in Eq. (1-1). Such a periodic function $f(\vec{r})$ can be expressed in terms of a Fourier series of the form

$$f(\vec{r}) = \sum_{\vec{K}_m} f_{\vec{K}_m} e^{i\vec{K}_m \cdot \vec{r}}, \quad (1-3)$$

where the $f_{\vec{K}_m}$'s, the Fourier coefficients, may be complex. The substi-

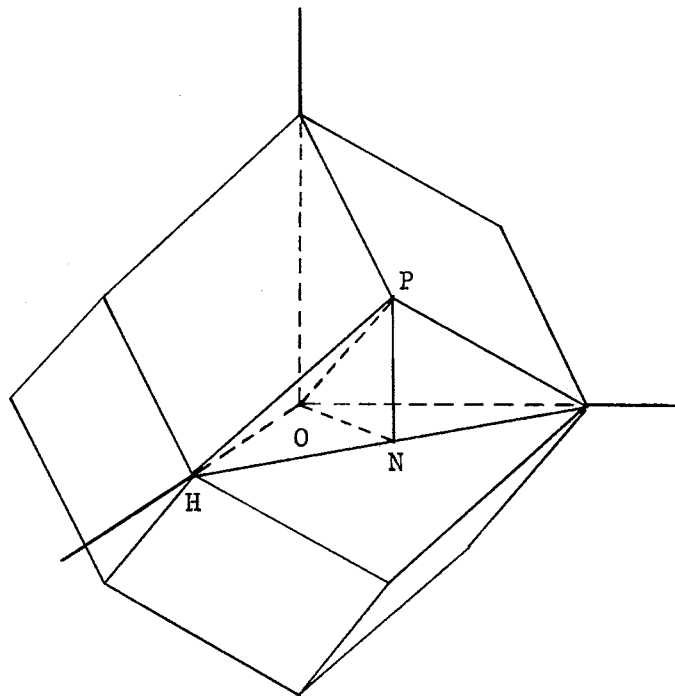


Figure 1. Wigner-Seitz Cell of the Face-Centered Cubic Lattice and the Fundamental Wedge

tution of Eq. (1-3) into Eq. (1-2) yields the requirement

$$\vec{K}_m \cdot \vec{a}_i = 2\pi m_i; \quad i = 1, 2, 3, \quad (1-4)$$

where the m_i are integers. Eq. (1-4) uniquely determines the allowed values of \vec{K}_m . These are given by

$$\vec{K}_m = m_1 \vec{b}_1 + m_2 \vec{b}_2 + m_3 \vec{b}_3, \quad (1-5)$$

where the m_i are integers and where

$$\vec{b}_i \cdot \vec{a}_j = 2\pi \delta_{ij}. \quad (1-6)$$

The symbol δ_{ij} is the Kronecker delta defined in the usual manner. This leads to the following set of relations

$$\begin{aligned} \vec{b}_1 &= \frac{2\pi \vec{a}_2 \times \vec{a}_3}{[\vec{a}_1 \vec{a}_2 \vec{a}_3]}, \\ \vec{b}_2 &= \frac{2\pi \vec{a}_3 \times \vec{a}_1}{[\vec{a}_1 \vec{a}_2 \vec{a}_3]}, \\ \vec{b}_3 &= \frac{2\pi \vec{a}_1 \times \vec{a}_2}{[\vec{a}_1 \vec{a}_2 \vec{a}_3]}, \end{aligned} \quad (1-7)$$

where $[\vec{a}_1 \vec{a}_2 \vec{a}_3] = |\vec{a}_1 \cdot (\vec{a}_2 \times \vec{a}_3)| = |\vec{a}_2 \cdot (\vec{a}_3 \times \vec{a}_1)| = |\vec{a}_3 \cdot (\vec{a}_1 \times \vec{a}_2)| = \Omega$

is the volume of the primitive unit cell mentioned earlier. The Fourier coefficients, $f_{\vec{K}_m}$, are given by

$$f_{\vec{K}_m} = \frac{1}{\Omega} \int_{\Omega} f(\vec{r}) e^{-i\vec{K}_m \cdot \vec{r}} d\tau, \quad (1-8)$$

where Ω is the volume of the primitive unit cell, and where the limits of integration are over the volume of a unit cell.

Eq. (1-8) can also be written as

$$f_{\vec{k}_m} = \frac{1}{N\Omega} \int_{N\Omega} f(\vec{r}) e^{-i\vec{k}_m \cdot \vec{r}} d\tau,$$

where the limits of integration are now over the volume of N unit cells.

The vectors \vec{b}_1 , \vec{b}_2 and \vec{b}_3 defined in Eq. (1-7) are called the basic primitive translations of the reciprocal lattice generated by the set of vectors \vec{k}_m , and the parallelepiped constructed from \vec{b}_1 , \vec{b}_2 , and \vec{b}_3 is called the primitive unit cell of the reciprocal lattice. For a face-centered cubic crystal such as copper, the primitive translations \vec{k}_m generate a body-centered cubic structure in reciprocal lattice space. The Wigner-Seitz cell of this reciprocal lattice is called the Brillouin zone and is shown in Figure 2.

D. Atomic Units

Throughout this investigation, Hartree atomic units are used. This system of units are established by defining unit of mass \equiv rest mass of electron; unit of length \equiv radius of first Bohr orbit of hydrogen atom; unit of charge \equiv magnitude of charge on electron; unit of energy \equiv twice the ionization energy of the normal state of the hydrogen atom.

Unless otherwise specified, all equations and numerical values that appear in this work are understood to be in this system of units.

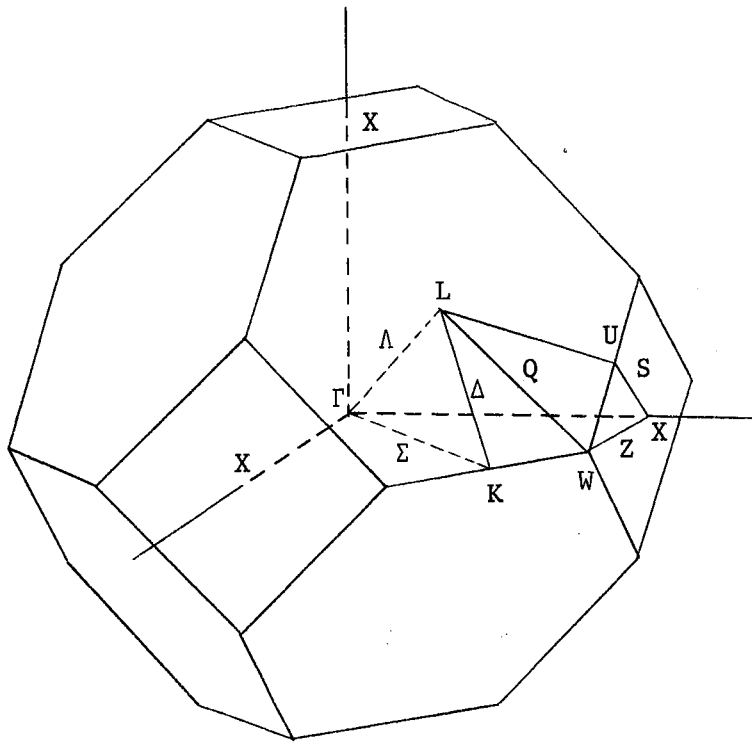


Figure 2. Brillouin Zone of Face-Centered Cubic Lattice

CHAPTER II

CRYSTAL POTENTIAL

A. General Description

In non-magnetic energy band calculations, each electron is considered as moving in a periodic potential field which has the same periodicity as that of the crystal under study. This potential is assumed to be the average effect of all electron-nuclei and electron-electron interactions. Due to this averaging, the potential experienced by each electron is only a function of its own position in the crystal and is not a function of the coordinates of the other electrons. Further, it is assumed that all electrons of the crystal experience the same potential.

The crystal potential, $V(\vec{r})$, used in this calculation is assumed to be represented by the sum of two contributions, the Coulomb portion denoted by $V^{\text{coul}}(\vec{r})$, and the exchange portion denoted by $V^{\text{exch}}(\vec{r})$. The crystal potential can thus be written as

$$V(\vec{r}) = V^{\text{coul}}(\vec{r}) + V^{\text{exch}}(\vec{r}) . \quad (2-1)$$

Unlike the approximations usually made about the crystal potential used in APW method, here it is not necessary to assume the muffin-tin form for the crystal potential.

The physical model adopted for the construction of $V(\vec{r})$ in this calculation is based on the assumption that the crystal charge density,

$\rho_{\text{crys}}(\vec{r})$, is obtained by a superposition of atomic charge densities, $\rho_{\text{atom}}(\vec{r})$, over all lattice sites in the crystal. This can be represented by the following equation

$$\rho_{\text{crys}}(\vec{r}) = \sum_{\vec{R}_\nu} \rho_{\text{atom}}(\vec{r} - \vec{R}_\nu), \quad (2-2)$$

where \vec{R}_ν is summed over all lattice sites.

Because of its periodic nature, the crystal potential can be expressed in a Fourier series as

$$V(\vec{r}) = \sum_{\vec{K}_\nu} V(\vec{K}_\nu) e^{i\vec{K}_\nu \cdot \vec{r}}, \quad (2-3)$$

where \vec{K}_ν is summed over all the reciprocal lattice vectors, and where the $V(\vec{K}_\nu)$ are the Fourier coefficients of the crystal potential. These Fourier coefficients, $V(\vec{K}_\nu)$, are given by

$$V(\vec{K}_\nu) = \frac{1}{N\Omega} \int_{\text{crys}} V(\vec{r}) e^{-i\vec{K}_\nu \cdot \vec{r}} d\tau, \quad (2-4)$$

where Ω is the volume of the primitive unit cell, and N represents, symbolically, the number of primitive cells in the crystal. Similarly, due to the periodicity of the crystal potential, and the model assumed, the Coulomb portion, $V^{\text{coul}}(\vec{r})$, and the exchange portion, $V^{\text{exch}}(\vec{r})$, can each be expressed individually in a Fourier series as

$$V^{\text{coul}}(\vec{r}) = \sum_{\vec{K}_\nu} V^{\text{coul}}(\vec{K}_\nu) e^{i\vec{K}_\nu \cdot \vec{r}}, \quad (2-5)$$

$$V^{\text{exch}}(\vec{r}) = \sum_{\vec{K}_\nu} V^{\text{exch}}(\vec{K}_\nu) e^{i\vec{K}_\nu \cdot \vec{r}}, \quad (2-6)$$

where the Fourier coefficients $V^{\text{coul}}(\vec{k}_\nu)$ and $V^{\text{exch}}(\vec{k}_\nu)$ are given by

$$V^{\text{coul}}(\vec{k}_\nu) = \frac{1}{N\Omega} \int_{\text{crys}} V^{\text{coul}}(\vec{r}) e^{-i\vec{k}_\nu \cdot \vec{r}} d\tau, \quad (2-7)$$

$$V^{\text{exch}}(\vec{k}_\nu) = \frac{1}{N\Omega} \int_{\text{crys}} V^{\text{exch}}(\vec{r}) e^{-i\vec{k}_\nu \cdot \vec{r}} d\tau. \quad (2-8)$$

In Eqs. (2-7) and (2-8) N and Ω have the same meaning as they stand in Eq. (2-4).

The existence of the inversion symmetry in fcc structure makes it possible for one to rewrite Eqs. (2-3), (2-4), (2-5), (2-6), (2-7), and (2-8) respectively into the forms given by Eqs. (2-9), (2-10), (2-11), (2-12), (2-13) and (2-14), i.e.,

$$V(\vec{r}) = \sum_{\vec{k}_\nu} V(\vec{k}_\nu) \cos \vec{k}_\nu \cdot \vec{r}, \quad (2-9)$$

$$V(\vec{k}_\nu) = \frac{1}{N\Omega} \int_{\text{crys}} V(\vec{r}) \cos(\vec{k}_\nu \cdot \vec{r}) d\tau \quad (2-10)$$

$$V^{\text{coul}}(\vec{r}) = \sum_{\vec{k}_\nu} V^{\text{coul}}(\vec{k}_\nu) \cos(\vec{k}_\nu \cdot \vec{r}), \quad (2-11)$$

$$V^{\text{exch}}(\vec{r}) = \sum_{\vec{k}_\nu} V^{\text{exch}}(\vec{k}_\nu) \cos(\vec{k}_\nu \cdot \vec{r}), \quad (2-12)$$

$$V^{\text{coul}}(\vec{k}_\nu) = \frac{1}{N\Omega} \int_{\text{crys}} V^{\text{coul}}(\vec{r}) \cos(\vec{k}_\nu \cdot \vec{r}) d\tau, \quad (2-13)$$

and

$$V^{\text{exch}}(\vec{k}_\nu) = \frac{1}{N\Omega} \int_{\text{crys}} V^{\text{exch}}(\vec{r}) \cos(\vec{k}_\nu \cdot \vec{r}) d\tau. \quad (2-14)$$

Employing the relations shown in Eqs. (2-9), (2-11), (2-12), and the uniqueness of the set of Fourier coefficients for a given periodic function one can then write

$$V(\vec{k}_\nu) = V^{\text{coul}}(\vec{k}_\nu) + V^{\text{exch}}(\vec{k}_\nu). \quad (2-15)$$

Only the Fourier coefficients, $V(\vec{k}_\nu)$, of the crystal potential, $V(\vec{r})$, are used in this calculation. In order to calculate $V(\vec{k}_\nu)$ one has to evaluate $V^{\text{coul}}(\vec{k}_\nu)$ and $V^{\text{exch}}(\vec{k}_\nu)$ first. This is carried out in the following Sections B and C.

B. Coulomb Potential

The coulomb portion of the crystal potential, $V^{\text{coul}}(\vec{r})$, is related to the crystal charge density, $\rho_{\text{crys}}^{\text{coul}}(\vec{r})$, through the Poisson's equation in the following manner

$$\nabla^2 V^{\text{coul}}(\vec{r}) = 4\pi\rho_{\text{crys}}^{\text{coul}}(\vec{r}), \quad (2-16)$$

where the crystal charge density is given by

$$\rho_{\text{crys}}^{\text{coul}}(\vec{r}) = \rho_{\text{crys}}^{\text{nuclear}}(\vec{r}) - \rho_{\text{crys}}^{\text{electronic}}(\vec{r}). \quad (2-17)$$

In Eq. (2-17) one has the following equations for $\rho_{\text{crys}}^{\text{nuclear}}(\vec{r})$ and $\rho_{\text{crys}}^{\text{electronic}}(\vec{r})$, i.e.,

$$\rho_{\text{crys}}^{\text{nuclear}}(\vec{r}) = Z \sum_{\vec{R}_\nu} \delta(\vec{r} - \vec{R}_\nu), \quad (2-18)$$

$$\rho_{\text{crys}}^{\text{electronic}}(\vec{r}) = \sum_{\vec{R}_\nu} \rho_{\text{atom}}^{\text{electronic}}(\vec{r} - \vec{R}_\nu). \quad (2-19)$$

where $\delta(\vec{r})$ is the delta function defined in the usual manner, and where the electronic contribution, $\rho_{\text{atom}}^{\text{electronic}}(\vec{r})$, to the crystal charge density will be discussed later.

Because of the periodicity of crystal potential, and the fact that the charge distributions determine in part the crystal potential, one can expand $\rho_{\text{crys}}^{\text{nuclear}}(\vec{r})$ in terms of a Fourier series, i.e., one can write

$$\rho_{\text{crys}}^{\text{nuclear}}(\vec{r}) = \sum_{\vec{K}_\nu} \eta^{\text{nuclear}}(\vec{K}_\nu) \cos \vec{K}_\nu \cdot \vec{r}, \quad (2-20)$$

where $\eta^{\text{nuclear}}(\vec{K}_\nu)$ is the Fourier coefficient of $\rho_{\text{crys}}^{\text{nuclear}}(\vec{r})$. Similarly, one can write

$$\rho_{\text{crys}}^{\text{elec}}(\vec{r}) = \sum_{\vec{K}_\nu} \eta^{\text{elec}}(\vec{K}_\nu) \cos \vec{K}_\nu \cdot \vec{r}, \quad (2-21)$$

where $\eta^{\text{elec}}(\vec{K}_\nu)$ is the Fourier coefficient of $\rho_{\text{crys}}^{\text{elec}}(\vec{r})$.

Employing Eqs. (2-20) and (2-21) in Eq. (2-17) one obtains

$$\rho_{\text{crys}}^{\text{coul}}(\vec{r}) = \sum_{\vec{K}_\nu} \eta^{\text{nuclear}}(\vec{K}_\nu) \cos \vec{K}_\nu \cdot \vec{r} - \sum_{\vec{K}_\nu} \eta^{\text{elec}}(\vec{K}_\nu) \cos \vec{K}_\nu \cdot \vec{r}. \quad (2-22)$$

Application of ∇^2 to $V^{\text{coul}}(\vec{r})$ given in Eq. (2-9) leads to the following relation:

$$\nabla^2 V^{\text{coul}}(\vec{r}) = - \sum_{\vec{K}_\nu} K_\nu^2 V^{\text{coul}}(\vec{K}_\nu) \cos \vec{K}_\nu \cdot \vec{r}, \quad (2-23)$$

where $K_\nu^2 = \vec{K}_\nu \cdot \vec{K}_\nu$.

Substituting $\nabla^2 V^{\text{coul}}(\vec{r})$ of Eq. (2-23) and $\rho_{\text{crys}}^{\text{coul}}(\vec{r})$ of Eq. (2-22) into Eq. (2-16) yields the following relation

$$-\sum_{\vec{K}_\nu} K_\nu^2 V^{\text{coul}}(\vec{K}_\nu) \cos \vec{K}_\nu \cdot \vec{r} = 4\pi \left[\sum_{\vec{K}_\nu} \eta^{\text{nuclear}}(\vec{K}_\nu) \cos \vec{K}_\nu \cdot \vec{r} - \sum_{\vec{K}_\nu} \eta^{\text{elec}}(\vec{K}_\nu) \cos \vec{K}_\nu \cdot \vec{r} \right]. \quad (2-24)$$

Due to the uniqueness of the Fourier coefficients in the expansion for a given periodic function, Eq. (2-24) implies that one can write

$$V^{\text{coul}}(\vec{K}_\nu) = - \frac{4\pi}{K_\nu^2} [\eta^{\text{nucl}}(\vec{K}_\nu) - \eta^{\text{elec}}(\vec{K}_\nu)] \quad (2-25)$$

The Fourier coefficients, $V^{\text{coul}}(\vec{K}_\nu)$, of the Coulomb portion of the crystal potential, $V^{\text{coul}}(\vec{r})$ can be readily found after $\eta^{\text{nucl}}(\vec{K}_\nu)$ and $\eta^{\text{elec}}(\vec{K}_\nu)$ are evaluated.

From Eqs. (2-19) and (2-20) one can write

$$\eta^{\text{nucl}}(\vec{K}_\nu) = \frac{Z}{N\Omega} \sum_{\vec{R}_\mu} \int_{\text{crys}} \delta(\vec{r}-\vec{R}_\nu) \cos(\vec{K}_\nu \cdot \vec{r}) d\tau. \quad (2-26)$$

Using the definition of the δ -function and Eq. (1-6) the quantity,

$\sum_{\vec{R}_\nu} \int_{\text{crys}} \delta(\vec{r}-\vec{R}_\nu) \cos(\vec{K}_\nu \cdot \vec{R}_\nu) d\tau$, can be shown to be equal to N . Eq.

(2-26) can therefore be rewritten as

$$\eta^{\text{nucl}}(\vec{K}_\nu) = \frac{Z}{\Omega}. \quad (2-27)$$

It is seen from Eq. (2-21) that $\eta^{\text{elec}}(\vec{K}_\nu)$ is given by the following equation

$$\eta^{\text{elec}}(\vec{K}_\nu) = \frac{1}{N\Omega} \int_{\text{crys}} \rho^{\text{elec}}(\vec{r}) \cos \vec{K}_\nu \cdot \vec{r} d\tau. \quad (2-28)$$

The electronic contribution to the crystal charge density, $\rho^{\text{elec}}(\vec{r})$, is approximated by superposing the atomic charge densities over all lattice sites using the following equation

$$\rho^{\text{elec}}_{\text{crys}}(\vec{r}) = \sum_{\vec{R}_\nu} \rho^{\text{elec}}_{\text{atom}}(|\vec{r} - \vec{R}_\nu|), \quad (2-29)$$

The electronic contribution to the atomic charge density, $\rho_{\text{atom}}^{\text{elec}}(\vec{r})$, of Eq. (2-29), assuming the spherical symmetry of the atomic charge distributions, is given by

$$\rho_{\text{atom}}^{\text{elec}}(r) = \sum_{n\ell} \frac{1}{4\pi r^2} [\lambda_{n\ell} P_{n\ell}^2(r)], \quad (2-30)$$

where $\lambda_{n\ell}$ is the occupation number of the $n\ell$ th orbital, and where $P_{n\ell}(r) = r R_{n\ell}(r)$ with $R_{n\ell}(r)$ being the normalized radial wave functions of copper. For the ground state configuration of the copper atom, $\rho_{\text{atom}}^{\text{elec}}(r)$ can be explicitly written as

$$\rho_{\text{atom}}^{\text{elec}}(r) = \frac{1}{4\pi r^2} [2P_{1s}^2(r) + 2P_{2s}^2(r) + 6P_{2p}^2(r) + 2P_{3s}^2(r) + 6P_{3p}^2(r) + 10P_{3d}^2(r) + P_{4s}^2(r)]. \quad (2-31)$$

The Hartree radial wave functions $P_{n\ell}(r)$ used are the analytic Hartree-Fock results taken from Clementi's Tables of Atomic Wave Functions⁽¹⁹⁾. Using Eq. (2-29), $\rho_{\text{crys}}^{\text{elec}}(\vec{r})$ is calculated and tabulated for 130 points with $x \geq y \geq z$ for each point in 1/48 the volume of the central Wigner-Seitz cell. This small volume enclosed in the polyhedron OPNH, (See Figure 1), is called a fundamental wedge. Convergence for $\rho_{\text{crys}}^{\text{elec}}(\vec{r})$ is reached after contributions from 135 neighboring atoms are included in the summation over the \vec{R}_V 's. The value of $\rho_{\text{crys}}^{\text{elec}}(\vec{r})$ at any point inside the Wigner-Seitz cell, but outside the fundamental wedge can be obtained by applying one of the 48 symmetry operations of the cubic group to an appropriate point inside the fundamental wedge. The evaluated values of $\rho_{\text{crys}}^{\text{elec}}(\vec{r})$ vs. \vec{r} are arranged into a tabular form. These tabulated values are then curve fitted according to the following equation

$$\rho_{\text{crys}}^{\text{elec}}(\vec{r}) = \sum_{\vec{R}_v=1}^N \sum_{i=1}^{i_m} \alpha_i r_v^{\beta_i} e^{-\gamma_i r_v} \quad (2-32)$$

where $r_v = |\vec{r} - \vec{R}_v|$, and where $i_m = 15$ is the number of α_i , β_i , and γ_i needed to achieve a reasonably good fit. Convergence of $\rho_{\text{crys}}^{\text{elec}}(\vec{r})$ within the central unit cell is reached when $N = 135$. The set of α_i 's, β_i 's and γ_i 's determined through the least-square curve fitting procedures along with a comparison of the tabular and fit of $\rho_{\text{crys}}^{\text{elec}}(\vec{r})$ vs. \vec{r} are listed in Tables I and II respectively.

Let the total electronic crystal charge be denoted by q , then one can write the following relation

$$q = 29N, \quad (2-33)$$

where N as usual represents the number of unit cells in the crystal.

From Eq. (2-32) one can also write the following

$$\begin{aligned} q &= \sum_{\vec{R}_v=1}^N \int_{\text{crys}} \sum_{i=1}^{i_m} \alpha_i r_v^{\beta_i} e^{-\gamma_i r_v} d\tau_v, \\ &= N \int \sum_{i=1}^{i_m} \alpha_i r^{\beta_i} e^{-\gamma_i r} d\tau, \end{aligned} \quad (2-34)$$

where $d\tau_v$ is a differential volume element referring \vec{R}_v as origin in the integration. It is noted from Eqs. (2-33) and (2-34) that the integral in Eq. (2-34) should have a value of 29. Indeed, a calculation of the integral is carried out, and its value is found to be 28.9987.

Using $\rho_{\text{crys}}^{\text{elec}}(\vec{r})$ of Eq. (2-32) with the set of α_i 's, β_i 's, and γ_i 's given in Table I in Eq. (2-28) one can write the following expression for $\eta^{\text{elec}}(\vec{K}_v)$.

$$\eta^{\text{elec}}(\vec{K}_v) = \frac{1}{N\Omega} \int_{\text{crys}} \sum_{\vec{R}_v} \sum_{i=1}^{i_m} \alpha_i r_v^{\beta_i} e^{-\gamma_i r_v} \cos(\vec{K}_v \cdot \vec{r}) d\tau_v. \quad (2-35)$$

TABLE I
PARAMETERS OF CHARGE DENSITY AND CUBE
ROOT OF CHARGE DENSITY CURVE FITTINGS

i	α_i	δ_i	β_i	γ_i
1	2.365257E 04	1.090022E 03	0.0	-5.000000E 01
2	-1.762831E 04	1.579487E 04	1.000000E 00	-5.000000E 01
3	1.202866E 06	1.041624E 05	2.000000E 00	-5.000000E 01
4	-1.080016E 05	-8.516750E 04	0.0	-2.000000E 01
5	-3.597556E 05	-3.375534E 05	1.000000E 00	-2.000000E 01
6	-1.146115E 06	-6.874513E 05	2.000000E 00	-2.000000E 01
7	1.128512E 05	1.114391E 05	0.0	-1.200000E 01
8	-3.019734E 05	-2.116944E 05	1.000000E 00	-1.200000E 01
9	5.101124E 05	6.298377E 05	2.000000E 00	-1.200000E 01
10	-1.248570E 04	-3.126054E 04	0.0	-6.000000E 00
11	2.055028E 04	4.840531E 04	1.000000E 00	-6.000000E 00
12	-1.369872E 04	-4.819461E 04	2.000000E 00	-6.000000E 00
13	6.002434E 02	3.925860E 03	0.0	-3.000000E 00
14	-4.174568E 02	-3.089820E 03	1.000000E 00	-3.000000E 00
15	7.806668E 01	6.633662E 02	2.000000E 00	-3.000000E 00

TABLE II
FIT OF CHARGE DENSITY

X	Y	Z	TABULAR	FIT
1.50000E-02	0.0	0.0	6.98677E 03	6.98677E 03
1.50000E-02	1.50000E-02	0.0	4.89710E 03	4.89714E 03
1.50000E-02	1.50000E-02	1.50000E-02	3.73871E 03	3.73871E 03
3.00000E-02	0.0	0.0	2.98588E 03	2.98588E 03
3.00000E-02	1.50000E-02	0.0	2.45591E 03	2.45591E 03
3.00000E-02	1.50000E-02	1.50000E-02	2.06384E 03	2.06382E 03
3.00000E-02	3.00000E-02	0.0	1.52784E 03	1.52785E 03
3.00000E-02	3.00000E-02	1.50000E-02	1.33895E 03	1.33897E 03
4.50000E-01	1.50000E-02	0.0	1.18520E 03	1.18521E 03
4.50000E-02	1.50000E-02	1.50000E-02	1.05840E 03	1.05841E 03
4.50000E-02	3.00000E-02	0.0	8.63630E 02	8.63622E 02
4.50000E-02	3.00000E-02	1.50000E-02	7.88054E 02	7.88073E 02
6.00000E-02	0.0	0.0	6.67790E 02	6.67783E 02
6.50000E-02	0.0	0.0	5.48718E 02	5.48713E 02
6.50000E-02	6.50000E-02	0.0	2.69642E 02	2.69623E 02
6.50000E-02	6.50000E-02	6.50000E-02	2.04484E 02	2.04490E 02
1.30000E-01	0.0	0.0	1.70751E 02	1.70768E 02
1.30000E-01	6.50000E-02	0.0	1.45678E 02	1.45684E 02
1.30000E-01	6.50000E-02	6.50000E-02	1.24973E 02	1.24975E 02
1.30000E-01	1.30000E-01	0.0	9.26352E 01	9.26267E 01
1.30000E-01	1.30000E-01	6.50000E-02	8.00661E 01	8.00561E 01
2.00000E-01	0.0	0.0	7.48725E 01	7.48630E 01
1.95000E-01	6.50000E-02	0.0	6.94298E 01	6.94178E 01
1.95000E-01	6.50000E-02	6.50000E-02	6.04316E 01	6.04236E 01
1.30000E-01	1.30000E-01	1.30000E-01	5.28162E 01	6.28142E 01
1.95000E-01	1.30000E-01	0.0	4.63655E 01	4.63706E 01
1.95000E-01	1.30000E-01	6.50000E-02	4.08941E 01	4.08994E 01
2.60000E-01	0.0	0.0	3.22915E 01	3.22985E 01
2.60000E-01	0.0	0.0	3.22915E 01	3.22985E 01
2.00000E-01	2.00000E-01	0.0	2.37278E 01	2.37332E 01
2.00000E-01	2.00000E-01	2.00000E-01	1.20515E 01	1.20373E 01

TABLE II (Continued)

X	Y	Z	TABULAR	FIT
4.00000E-01	0.0	0.0	8.81597E 00	8.80584E 00
4.00000E-01	2.00000E-01	0.0	7.57176E 00	7.57498E 00
4.00000E-01	2.00000E-01	2.00000E-01	6.81256E 00	6.82299E 00
4.00000E-01	4.00000E-01	0.0	5.58400E 00	5.58997E 00
4.00000E-01	4.00000E-01	2.00000E-01	5.02885E 00	5.02933E 00
6.00000E-01	2.00000E-01	0.0	4.51501E 00	4.51134E 00
6.00000E-01	2.00000E-01	2.00000E-01	4.04642E 00	4.04045E 00
6.00000E-01	4.00000E-01	0.0	3.24640E 00	3.24115E 00
6.00000E-01	4.00000E-01	2.00000E-01	2.91057E 00	2.90735E 00
7.58989E-01	3.79494E-01	0.0	1.91004E 00	1.91548E 00
7.58989E-01	3.79494E-01	3.79494E-01	1.34396E 00	1.35157E 00
7.58989E-01	7.58989E-01	0.0	7.21075E-01	7.22513E-01
7.58989E-01	7.58989E-01	3.79494E-01	5.47802E-01	5.46178E-01
1.13848E 00	3.79494E-01	0.0	4.25097E-01	4.21715E-01
1.13848E 00	3.79494E-01	3.79494E-01	3.36440E-01	3.32663E-01
1.13848E 00	7.58989E-01	0.0	2.21945E-01	2.19663E-01
1.13848E 00	7.58989E-01	3.79494E-01	1.84405E-01	1.83350E-01
1.13848E 00	7.58989E-01	7.58989E-01	1.14282E-01	1.16145E-01
1.13848E 00	1.13848E 00	0.0	9.98682E-02	1.02006E-01
1.13848E 00	1.13848E 00	3.79494E-01	8.79371E-02	9.04078E-02
1.13848E 00	1.13848E 00	7.58989E-01	6.32862E-02	6.57274E-02
1.51798E 00	7.58989E-01	7.58989E-01	5.27747E-02	5.45632E-02
1.51798E 00	1.13848E 00	0.0	4.92946E-02	5.03077E-02
1.51798E 00	1.51798E 00	3.79494E-01	3.25837E-02	3.12375E-02
1.51798E 00	1.51798E 00	7.58989E-01	2.88492E-02	2.77500E-02
1.89747E 00	1.51798E 00	0.0	2.91738E-02	2.69319E-02
1.89747E 00	1.51798E 00	3.79494E-01	2.81734E-02	2.61466E-02
1.89747E 00	1.51798E 00	7.58989E-01	2.57781E-02	2.43888E-02
1.89747E 00	1.51798E 00	1.13848E 00	2.33169E-02	2.28012E-02
2.65646E 00	3.79494E-01	0.0	1.91771E-02	1.93933E-02
2.65646E 00	3.79494E-01	3.79494E-01	1.93501E-02	1.95130E-02
2.65646E 00	7.58989E-01	0.0	2.03550E-02	2.00872E-02

TABLE II (Continued)

X	Y	Z	TABULAR	FIT
2.65646E 00	7.58989E-01	3.79494E-01	2.03631E-02	2.01407E-02
2.65646E 00	7.58989E-01	7.58989E-01	2.08280E-02	2.04984E-02
3.03595E 00	0.0	0.0	1.65739E-02	1.78168E-02
3.03595E 00	3.79494E-01	0.0	1.70795E-02	1.81090E-02
3.03595E 00	3.79494E-01	3.79494E-01	1.75110E-02	1.83736E-02
3.41540E 00	0.0	0.0	1.59840E-02	1.74926E-02

Carrying out the integration for each lattice site \vec{R}_v and summing them up, the above equation becomes

$$\eta^{\text{elec}}(\vec{K}_v) = \frac{1}{\Omega} \sum_{i=1}^{i_m} \int \alpha_i r^{\beta_i} e^{-\gamma_i r} \cos(\vec{K}_v \cdot \vec{r}) r^2 \sin\theta \, d\theta \, d\phi \, dr.$$

If one lets θ to be the angle between the vector \vec{K}_v and \vec{r} , i.e., chooses the z-axis in the direction of the vector \vec{K}_v , Eq. (2-35) can then be written as

$$\eta^{\text{elec}}(\vec{K}_v) = \frac{1}{\Omega} \sum_{i=1}^{i_m} \int_{\text{crys}} \alpha_i r^{\beta_i} e^{-\gamma_i r} \cos(K_v r \cos\theta) r^2 \sin\theta \, d\theta \, d\phi \, dr. \quad (2-36)$$

Eq. (2-36) through a few steps of simplification, can be put into the following form

$$\eta^{\text{elec}}(\vec{K}_v) = \frac{4\pi}{K_v \Omega} \sum_{i=1}^{i_m} \int_0^\infty \alpha_i r^{\beta_i+1} e^{-\gamma_i r} \sin(K_v r) \, dr, \quad (2-37)$$

Using $\eta^{\text{nucl}}(\vec{K}_v)$ of Eq. (2-27) and $\eta^{\text{elec}}(\vec{K}_v)$ of Eq. (2-35) in Eq. (2-25) one finally obtains for $V^{\text{coul}}(\vec{K}_v)$ the following expression

$$V^{\text{coul}}(\vec{K}_v) = -\frac{4\pi}{K_v^2 \Omega} \left[Z - \frac{4\pi}{K_v} \sum_{i=1}^{i_m} \int_0^\infty \alpha_i r^{\beta_i+1} e^{-\gamma_i r} \sin(K_v r) \, dr \right] \quad (2-38)$$

C. The Exchange Potential

The exchange portion of the crystal potential, $V^{\text{exch}}(\vec{r})$, needed to calculate $V^{\text{exch}}(\vec{K}_v)$ by using Eq. (2-14) is obtained by adopting Slater's free-electron gas approximation⁽²⁰⁾. According to this scheme $V^{\text{exch}}(\vec{r})$ can be approximated by the following equation:

$$V^{\text{exch}}(\vec{r}) = -3 \left[\frac{3}{8\pi} \rho_{\text{crys}}^{\text{elec}}(\vec{r}) \right]^{1/3}, \quad (2-39)$$

where $\rho_{\text{crys}}^{\text{elec}}(\vec{r})$ is given by Eq. (2-29).

In order to compute $V^{\text{exch}}(\vec{K}_\nu)$, the quantity $[\rho_{\text{crys}}^{\text{elec}}(\vec{r})]^{1/3}$ is evaluated, and tabulated over the same fundamental wedge discussed in the previous Section B. The tabular data is then curve fitted in the same manner as discussed previously using the analytic form

$$[\rho_{\text{crys}}^{\text{elec}}(\vec{r})]^{1/3} = \sum_{\vec{R}_\nu=1}^N \sum_{i=1}^{i_m} \delta_i r_\nu^{\beta_i} e^{-\gamma_i r_\nu}, \quad (2-40)$$

where again $r_\nu = |\vec{r} - \vec{R}_\nu|$. Also in Eq. (2-40) i_m , β_i , and γ_i all have the same meaning as they stand in Eq. (2-32). The set of values of δ_i 's are listed in the second column of Table I. For comparison the tabular data and the results of the curve fitting are listed in Table III.

Utilizing Eqs. (2-40) and (2-39) in Eq. (2-14) one obtains the following expression.

$$V^{\text{exch}}(\vec{K}_\mu) = -\frac{3}{N\Omega} \left(\frac{3}{8\pi}\right)^{1/3} \int_{\text{crys}} \left(\sum_{\vec{R}_\nu}^N \sum_{i=1}^{i_m} \delta_i r_\nu^{\beta_i} e^{-\gamma_i r_\nu} \right) \cos(\vec{K}_\mu \cdot \vec{r}) d\tau_\nu. \quad (2-41)$$

In a manner similar to that described for simplifying Eq. (2-36) the above equation can be put into the form

$$V^{\text{exch}}(\vec{K}_\mu) = -\frac{12\pi}{K_\mu \Omega} \left(\frac{3}{8\pi}\right)^{1/3} \sum_{i=1}^{i_m} \int_0^\infty \delta_i r^{\beta_i+1} e^{-\gamma_i r} \sin(K_\mu r) dr. \quad (2-42)$$

D. The Fourier Coefficients of Crystal Potential

The Fourier coefficients of the crystal potential, $V(\vec{K}_\nu)$, can finally be written down by substituting Eqs. (2-38) and (2-42) into

TABLE III
FIT OF CUBE ROOT OF CHARGE DENSITY

X	Y	Z	TABULAR	FIT
1.50000E-02	0.0	0.0	1.91172E 01	1.90983E 01
1.50000E-02	1.50000E-02	0.0	1.69816E 01	1.69539E 01
1.50000E-02	1.50000E-02	1.50000E-02	1.55205E 01	1.54967E 01
3.00000E-02	0.0	0.0	1.43998E 01	1.43868E 01
3.00000E-02	1.50000E-02	0.0	1.34918E 01	1.34832E 01
3.00000E-02	1.50000E-02	1.50000E-02	1.27319E 01	1.27182E 01
3.00000E-02	3.00000E-02	0.0	1.15175E 01	1.15050E 01
3.00000E-02	3.00000E-02	1.50000E-02	1.10218E 01	1.10130E 01
4.50000E-02	1.50000E-02	0.0	1.05827E 01	1.05666E 01
4.50000E-02	1.50000E-02	1.50000E-02	1.01910E 01	1.01778E 01
4.50000E-02	3.00000E-02	0.0	9.52304E 00	9.49047E 00
4.50000E-02	3.00000E-02	1.50000E-02	9.23673E 00	9.23013E 00
6.00000E-02	0.0	0.0	8.74070E 00	8.72276E 00
6.50000E-02	0.0	0.0	8.18684E 00	8.18244E 00
6.50000E-02	6.50000E-02	0.0	6.46044E 00	6.46904E 00
6.50000E-02	6.50000E-02	6.50000E-02	5.89142E 00	5.88353E 00
1.30000E-01	0.0	0.0	5.54780E 00	5.53481E 00
1.30000E-01	6.50000E-02	0.0	5.26175E 00	5.25008E 00
1.30000E-01	6.50000E-02	6.50000E-02	4.99964E 00	5.00020E 00
1.30000E-01	1.30000E-01	0.0	4.52472E 00	4.52886E 00
1.30000E-01	1.30000E-01	6.50000E-02	4.31006E 00	4.31359E 00
2.00000E-01	0.0	0.0	4.21477E 00	4.22007E 00
1.95000E-01	6.50000E-02	0.0	4.11006E 00	4.11325E 00
1.95000E-01	6.50000E-02	6.50000E-02	3.92423E 00	3.92328E 00
1.30000E-01	1.30000E-01	1.30000E-01	3.75194E 00	3.74977E 00
1.95000E-01	1.30000E-01	0.0	3.59251E 00	3.59251E 00
1.95000E-01	1.30000E-01	6.50000E-02	3.44524E 00	3.43994E 00
2.60000E-01	0.0	0.0	3.18441E 00	3.17765E 00
2.60000E-01	0.0	0.0	3.18441E 00	3.17765E 00
2.00000E-01	2.00000E-01	0.0	2.87355E 00	2.87137E 00
2.00000E-01	2.00000E-01	2.00000E-01	2.29270E 00	2.30397E 00

TABLE III (Continued)

X	Y	Z	TABULAR	FIT
4.00000E-01	0.0	0.0	2.06581E 00	2.07201E 00
4.00000E-01	2.00000E-01	0.0	1.96366E 00	1.96016E 00
4.00000E-01	2.00000E-01	2.00000E-01	1.89570E 00	1.88737E 00
4.00000E-01	4.00000E-01	0.0	1.77411E 00	1.76950E 00
4.00000E-01	4.00000E-01	2.00000E-01	1.71326E 00	1.71288E 00
6.00000E-01	2.00000E-01	0.0	1.65280E 00	1.65573E 00
6.00000E-01	2.00000E-01	2.00000E-01	1.59352E 00	1.59894E 00
6.00000E-01	4.00000E-01	0.0	1.48070E 00	1.48662E 00
6.00000E-01	4.00000E-01	2.00000E-01	1.42777E 00	1.43246E 00
7.58989E-01	3.79494E-01	0.0	1.24074E 00	1.23562E 00
7.58989E-01	3.79494E-01	3.79494E-01	1.10356E 00	1.09258E 00
7.58989E-01	7.58989E-01	0.0	8.96727E-01	8.90896E-01
7.58989E-01	7.58989E-01	3.79494E-01	8.18228E-01	8.18849E-01
1.13848E 00	3.79494E-01	0.0	7.51905E-01	7.55868E-01
1.13848E 00	3.79494E-01	3.79494E-01	6.95509E-01	7.03759E-01
1.13848E 00	7.58989E-01	0.0	6.05455E-01	6.15843E-01
1.13848E 00	7.58989E-01	3.79494E-01	5.69191E-01	5.77694E-01
1.13848E 00	7.58989E-01	7.58989E-01	4.85281E-01	4.83976E-01
1.13848E 00	1.13848E 00	0.0	4.63955E-01	4.59928E-01
1.13848E 00	1.13848E 00	3.79494E-01	4.44690E-01	4.37624E-01
1.13848E 00	1.13848E 00	7.58989E-01	3.98507E-01	3.86325E-01
1.51798E 00	7.58989E-01	7.58989E-01	3.75095E-01	3.60486E-01
1.51798E 00	1.13848E 00	0.0	3.66663E-01	3.53910E-01
1.51798E 00	1.51798E 00	3.79494E-01	3.19399E-01	3.20503E-01
1.51798E 00	1.51798E 00	7.58989E-01	3.06698E-01	3.15234E-01
1.89747E 00	1.51798E 00	0.0	3.07844E-01	3.13736E-01
1.89747E 00	1.51798E 00	3.79494E-01	3.04284E-01	3.12877E-01
1.89747E 00	1.51798E 00	7.58989E-01	2.95405E-01	3.11304E-01
1.89747E 00	1.51798E 00	1.13848E 00	2.85687E-01	3.10474E-01
2.65646E 00	3.79494E-01	0.0	2.67667E-01	2.60554E-01
2.65646E 00	3.79494E-01	3.79494E-01	2.68469E-01	2.64902E-01
2.65646E 00	7.58989E-01	0.0	2.73039E-01	2.72546E-01

TABLE III (Continued)

X	Y	Z	TABULAR	FIT
2.65646E 00	7.58989E-01	3.79494E-01	2.73075E-01	2.75964E-01
2.65646E 00	7.58989E-01	7.58989E-01	2.75137E-01	2.84740E-01
3.03595E 00	0.0	0.0	2.54962E-01	2.40772E-01
3.03595E 00	3.79494E-01	0.0	2.57528E-01	2.46389E-01
3.03595E 00	3.79494E-01	3.79494E-01	2.59679E-01	2.51646E-01
3.41540E 00	0.0	0.0	2.51900E-01	2.34803E-01

Eq. (2-15).

$$\begin{aligned}
 V(\vec{K}_V) = & -\frac{4\pi}{K_V^2 \Omega} \left[Z - \frac{4\pi}{K_V} \sum_{i=1}^{i_m} \int_0^\infty \alpha_i r^{\beta_i+1} e^{-\gamma_i r} \sin(K_V r) dr \right. \\
 & \left. + 3K_V \sum_{i=1}^{i_m} \int_0^\infty \left(\frac{3}{8\pi}\right)^{1/3} \delta_i r^{\beta_i+1} e^{-\gamma_i r} \sin(K_V r) dr \right].
 \end{aligned}
 \tag{2-43}$$

The Fourier coefficients, $V(\vec{K}_V)$, are calculated according to Eq. (2-43), and are then tabulated. Part of the calculated $V(\vec{K}_V)$'s are listed in Table IV.

TABLE IV

THE FIRST EIGHTY OF THE FOURIER COEFFICIENTS, $V(\vec{K}_V)$, OF
THE CRYSTAL POTENTIAL, $V(\vec{r})$, ARE LISTED IN THIS TABLE

$\frac{a}{2\pi} \vec{K}_V = \vec{L}$			Fourier Coefficients
L_x	L_y	L_z	$V(\vec{K}_V)$
0	0	0	-0.10000E 01
1	1	1	-0.54677E 00
2	0	0	-0.47232E 00
2	2	0	-0.32565E 00
3	1	1	-0.26562E 00
2	2	2	-0.25023E 00
4	0	0	-0.20412E 00
3	3	1	-0.18042E 00
4	2	0	-0.17387E 00
4	2	2	-0.15228E 00
3	3	3	-0.13948E 00
5	1	1	-0.13948E 00
4	4	0	-0.12226E 00
5	3	1	-0.11373E 00
4	4	2	-0.11112E 00
6	0	0	-0.11112E 00
6	2	0	-0.10171E 00
5	3	3	-0.95594E 01
6	2	2	-0.93707E 01
4	4	4	-0.86837E 01
5	5	1	-0.82314E 01
7	1	1	-0.82314E 01
6	4	0	-0.80911E 01
6	4	2	-0.75768E 01
5	5	3	-0.72342E 01
7	3	1	-0.72342E 01
8	0	0	-0.67320E 01
7	3	3	-0.64654E 01
6	4	4	-0.63817E 01
8	2	0	-0.63817E 01
6	6	0	-0.60691E 01
8	2	2	-0.60691E 01
7	5	1	-0.58559E 01
5	5	5	-0.58559E 01

TABLE IV (Continued)

$\frac{a_0}{2\pi} \vec{K}_v = \vec{L}$			Fourier Coefficients
L_x	L_y	L_z	$V(\vec{K}_v)$
6	6	2	-0.57884E 01
8	4	0	-0.55345E 01
7	5	3	-0.53594E 01
9	1	1	-0.53594E 01
8	4	2	-0.53037E 01
6	6	4	-0.50925E 01
9	3	1	-0.49455E 01
8	4	4	-0.47193E 01
7	5	5	-0.45936E 01
7	7	1	-0.45936E 01
9	3	3	-0.45936E 01
8	6	0	-0.45532E 01
10	0	0	-0.45532E 01
8	6	2	-0.43987E 01
10	2	0	-0.43987E 01
7	7	3	-0.42896E 01
9	5	1	-0.42896E 01
6	6	6	-0.42545E 01
10	2	2	-0.42545E 01
9	5	3	-0.40238E 01
8	6	4	-0.39929E 01
10	4	0	-0.39929E 01
10	4	2	-0.38738E 01
7	7	5	-0.37891E 01
11	1	1	-0.37891E 01
8	8	0	-0.36558E 01
9	5	5	-0.35802E 01
9	7	1	-0.35802E 01
11	3	1	-0.35802E 01
8	8	2	-0.35557E 01
10	4	4	-0.35557E 01
8	6	6	-0.34609E 01
10	6	0	-0.34609E 01
9	7	3	-0.33931E 01
11	3	3	-0.33931E 01
10	6	2	-0.33710E 01
8	8	4	-0.32857E 01
12	0	0	-0.32857E 01
7	7	7	-0.32245E 01
11	5	1	-0.32245E 01
12	2	0	-0.32046E 01
10	6	4	-0.31274E 01
12	2	2	-0.31274E 01
11	5	3	-0.30719E 01
9	7	5	-0.30719E 01

TABLE IV (Continued)

$\frac{a_0}{2\pi} \vec{K}_v = \vec{L}$			Fourier Coefficients
L_x	L_y	L_z	$V(\vec{K}_v)$
12	4	0	-0.29837E 01

CHAPTER III

TIGHT-BINDING BASIS FUNCTIONS

An acceptable crystalline wave function must have certain transformation properties required by translational and rotational symmetry of the crystal lattice. The set of basis functions chosen for this investigation are the Bloch sums, $b_{n\ell m}(\vec{k}, \vec{r})$, constructed in the following manner

$$b_{n\ell m}(\vec{k}, \vec{r}) = \frac{1}{\sqrt{N}} \sum_{\vec{R}_\nu} e^{i\vec{k} \cdot \vec{R}_\nu} \phi_{n\ell m}(\vec{r} - \vec{R}_\nu), \quad (3-1)$$

where N represents, symbolically, the number of unit cells in the crystal, \vec{k} labels the irreducible representation of the translation group to which $b_{n\ell m}(\vec{k}, \vec{r})$ belongs and where the indices, n , ℓ , and m label the n th occurrence of the m th partner of the ℓ th irreducible representation of the three dimensional rotation group $O(3)$ to which the $\phi_{n\ell m}(\vec{r})$ belong.

As will be seen shortly, $\phi_{n\ell m}(\vec{r})$ are chosen to be the self-consistent field (SCF) atomic wave functions. Since the highest symmetry possible in the group of the wave vector is that of the point group of the crystal, a subgroup of $O(3)$, all operations present in the group of the wave vector are also contained in $O(3)$. In order for the $b_{n\ell m}(\vec{k}, \vec{r})$ to form an acceptable set of basis functions for any and all points in the Brillouin zone, it is necessary for each and every value of \vec{k} to combine the given set of Bloch sums in such a manner that the periodic portion of this combination transforms as the desired member of

some particular irreducible representation of the group of the wave vector. Since any given group of the wave vector is a subgroup of $O(3)$, this condition will be satisfied if sufficient values of l are represented in the Bloch set and if all the $2l + 1$ values of m are included for each choice of l .

The functions $b_{n\ell m}(\vec{k}, \vec{r})$ can be shown to have the required transformation properties under translation by direct examination,

$$b_{n\ell m}(\vec{k}, \vec{r} + \vec{R}_\nu) = \frac{1}{\sqrt{N}} \sum_{\vec{R}_\nu} e^{i\vec{k} \cdot \vec{R}_\nu} \phi_{n\ell m}(\vec{r} + \vec{R}_\nu, -\vec{R}_\nu), \quad (3-2)$$

where \vec{R}_ν is any translation vector. By multiplying and dividing its right hand side by $e^{i\vec{k} \cdot \vec{R}_\nu}$, the above expression can be rewritten

$$\begin{aligned} b_{n\ell m}(\vec{k}, \vec{r} + \vec{R}_\nu) &= \frac{1}{\sqrt{N}} e^{i\vec{k} \cdot \vec{R}_\nu} \sum_{\vec{R}_\nu} e^{i\vec{k} \cdot (\vec{R}_\nu - \vec{R}_\nu)} \phi_{n\ell m}[\vec{r} - (\vec{R}_\nu - \vec{R}_\nu)] \\ &= \frac{1}{\sqrt{N}} e^{i\vec{k} \cdot \vec{R}_\nu} b_{n\ell m}(\vec{k}, \vec{r}). \end{aligned} \quad (3-3)$$

Eq. (3-3) demonstrates the fact that the functions $b_{n\ell m}(\vec{k}, \vec{r})$ obey the Bloch condition and thus possess the required transformation properties under translation.

The transformation properties of $b_{n\ell m}(\vec{k}, \vec{r})$ under the coordinate operations R of the group of the wave vector can be examined in the following manner.

Let P_R represent the function operator corresponding to R defined in the usual manner^(21,22),

$$P_R f(\vec{r}) = f(R^{-1}\vec{r}). \quad (3-4)$$

The result of operating on $b_{n\ell m}(\vec{k}, \vec{r})$ by P_R can then be written as

$$P_R b_{n\ell m}(\vec{k}, \vec{r}) = \frac{1}{\sqrt{N}} \sum_{\vec{R}_v} e^{i\vec{k} \cdot \vec{R}_v} \phi_{n\ell m}(R^{-1} \vec{r} - \vec{R}_v). \quad (3-5)$$

All operations R of the group of the wave vector will leave the crystal invariant, since the group of the wave vector is a subgroup of the point group of the crystal. Thus when R operates on a translation vector \vec{R}_v , the result of the operation is another translation vector, say $\vec{R}_{v'}$, i.e.,

$$R \vec{R}_v = \vec{R}_{v'}. \quad (3-6)$$

Thus, Eq. (3-5) can be rewritten

$$P_R b_{n\ell m}(\vec{k}, \vec{r}) = \frac{1}{\sqrt{N}} \sum_{\vec{R}_v} e^{i\vec{k} \cdot R^{-1} \vec{R}_v} \phi_{n\ell m}(R^{-1}(\vec{r} - \vec{R}_v)). \quad (3-7)$$

Now, since applying the same orthogonal transformation, of which R is one, to both vectors in a scalar product does not alter the value of the product, one obtains

$$\begin{aligned} e^{i\vec{k} \cdot R^{-1} \vec{R}_v} &= e^{iR\vec{k} \cdot R(R^{-1} \vec{R}_v)} \\ &= e^{iR\vec{k} \cdot \vec{R}_v}. \end{aligned} \quad (3-8)$$

Thus, using the fact that R is a member of the group of the wave vector, i.e., using $R\vec{k} = \vec{k}$ in Eq. (3-8), it can thus be rewritten

$$e^{i\vec{k} \cdot R^{-1} \vec{R}_v} = e^{i\vec{k} \cdot \vec{R}_v}. \quad (3-9)$$

Using the above relation, Eq. (3-7) becomes

$$P_R b_{n\ell m}(\vec{k}, \vec{r}) = \frac{1}{\sqrt{N}} \sum_{\vec{R}_v} e^{i\vec{k} \cdot \vec{R}_v} \phi_{n\ell m}(R^{-1}(\vec{r} - \vec{R}_v)) \quad (3-10)$$

Eq. (3-10) indicates that the $b_{n\ell m}(\vec{k}, \vec{r})$ possess the same transformation

properties as $\phi_{n\ell m}(\vec{r})$ under the operations of the group of the wave vector.

To construct an acceptable set of basis functions with $b_{n\ell m}(\vec{k}, \vec{r})$ for any and all points in the Brillouin zone it is necessary for each and every value of \vec{k} to combine the given Bloch sums in such a way that this combination transforms as the desired partner of some particular irreducible representation of the group of the wave vector. This condition will be satisfied if sufficient values of ℓ are represented in the Bloch set and if all the $2\ell + 1$ values of m are included for each choice of ℓ , since any given group of the wave vector is a subgroup of the three-dimensional rotation group $O(3)$. The reduction of the irreducible representations of $O(3)$ in various point groups are available in standard references⁽²³⁾.

Recognizing the fact that the spherical harmonics $Y_{\ell}^m(\theta, \phi)$ form a basis of the irreducible representations of $O(3)$ the $b_{n\ell m}(\vec{k}, \vec{r})$ functions can be written as

$$b_{n\ell m}(\vec{k}, \vec{r}) = \frac{1}{\sqrt{N}} \sum_{\vec{R}_v} e^{i\vec{k} \cdot \vec{R}_v} \phi_{n\ell}(|\vec{r} - \vec{R}_v|) Y_{\ell}^m(\theta_v, \phi_v). \quad (3-11)$$

The choice of the proper $\phi_{n\ell}(\vec{r})$ functions is entirely left to the decision of the investigator, since this choice of $\phi_{n\ell}(\vec{r})$ is not dictated by symmetry. However, it is desirable that these $\phi_{n\ell}(\vec{r})$ are to be chosen in such a way to keep the number of basis functions to a minimum and yet the same time to give a reasonably good approximation of the desired wave functions for any given point in the Brillouin zone.

Since the main purpose of this investigation is to develop and extend the Gaussian orbital formulation of tight-binding to the d orbitals,

with particular emphasis on the so-called "d-bands" of the transition elements, the core states and the 4s-4p band are not included in this calculation. However, for a more detailed calculation the core states, the 4s states and the unoccupied 4p orbitals should all be included in forming the Bloch functions to introduce a rigorous variational solution of the secular equation.

The justification of ignoring the core states is that the 3d states are tightly bound. This can be seen by looking at some of the single-center and two-center overlap integrals between all possible pairs of the $3d_{xy}$, $3d_{yz}$, $3d_{zx}$, $3d_{x^2}$, $3d_{y^2}$, and $3d_{z^2}$ orbitals as listed in Table V. Tightly bound 3d states and narrow 3d bands are also predicted by the energy band calculations performed by L. F. Mattheiss⁽²⁴⁾ for the iron transition series solids. The addition of non muffin-tin terms should not destroy this gross effect and narrow bands are consistent with a tightly bound formalism, thus one should expect a tight-binding approach to give a reasonably accurate description of the d-band with the exception of s-p hybridization.

For this calculation the basis functions are chosen to be the Bloch sums constructed by using the 3d atomic orbitals of copper in the following manner:

$$b_{3dxy}(\vec{k}, \vec{r}) = \frac{1}{\sqrt{N}} \sum_{\vec{R}_\nu} e^{i\vec{k} \cdot \vec{R}_\nu} \phi_{3dxy}(\vec{r} - \vec{R}_\nu), \quad (3-12)$$

$$b_{3dyz}(\vec{k}, \vec{r}) = \frac{1}{\sqrt{N}} \sum_{\vec{R}_\nu} e^{i\vec{k} \cdot \vec{R}_\nu} \phi_{3dyz}(\vec{r} - \vec{R}_\nu), \quad (3-13)$$

$$b_{3dzx}(\vec{k}, \vec{r}) = \frac{1}{\sqrt{N}} \sum_{\vec{R}_\nu} e^{i\vec{k} \cdot \vec{R}_\nu} \phi_{3dzx}(\vec{r} - \vec{R}_\nu), \quad (3-14)$$

TABLE V

VALUES OF THE SINGLE CENTER AND MULTICENTER INTEGRALS $\langle \phi_i(0) | \phi_j(\vec{B}) \rangle$; WHERE i AND j EACH RUNS OVER THE ORBITAL INDICES $3d_{xy}$, $3d_{yz}$; $3d_{zx}$, $3d_x^2$, $3d_y^2$; and $3d_z^2$, FOR THE FIRST TEN \vec{B} 's ARE LISTED IN THIS TABLE. THE VALUE OF A SPECIFIC INTEGRAL $\langle \phi_i(0) | \phi_j(\vec{B}) \rangle$ APPEARS AT THE INTERSECTION OF THE i th ROW AND j th COLUMN IN THE TABLE

$$\frac{2}{a_0} \vec{B} = (0,0,0)$$

9.99919E-01	0.0	0.0	0.0	0.0	0.0
0.0	9.99919E-01	0.0	0.0	0.0	0.0
0.0	0.0	9.99919E-01	0.0	0.0	0.0
0.0	0.0	0.0	9.99919E-01	3.33306E-01	3.33306E-01
0.0	0.0	0.0	3.33306E-01	9.99919E-01	3.33306E-01
0.0	0.0	0.0	3.33306E-01	3.33306E-01	9.99919E-01

$$\frac{2}{a_0} \vec{B} = (1,1,0)$$

2.04070E-02	0.0	0.0	2.28907E-02	2.28907E-02	1.34389E-02
0.0	-7.76875E-03	-1.18048E-02	0.0	0.0	0.0
0.0	-1.18048E-02	-7.76875E-03	0.0	0.0	0.0
2.28907E-02	0.0	0.0	1.71411E-02	3.01901E-02	9.10429E-03

TABLE V (Continued)

2.28907E-02	0.0	0.0	3.01901E-02	1.71411E-02	9.10429E-03
1.34389E-02	0.0	0.0	9.10427E-03	9.10427E-03	4.03605E-03
$\frac{2}{a_0} \vec{B} = (2,0,0)$					
-2.61836E-03	0.0	0.0	0.0	0.0	0.0
0.0	3.39626E-04	0.0	0.0	0.0	0.0
0.0	0.0	-2.61836E-03	0.0	0.0	0.0
0.0	0.0	0.0	9.30550E-03	1.91682E-03	1.91682E-03
0.0	0.0	0.0	1.91682E-03	3.39627E-04	1.13209E-04
0.0	0.0	0.0	1.91682E-03	1.13209E-04	3.39627E-04
$\frac{2}{a_0} \vec{B} = (2,1,1)$					
3.03420E-04	1.72025E-04	6.00308E-04	7.48974E-04	1.55116E-04	3.52385E-04
1.72025E-04	4.53828E-05	1.72025E-04	4.73121E-04	7.75582E-05	7.75582E-05
6.00308E-04	1.72025E-04	3.03420E-04	7.48974E-04	3.52385E-04	1.55116E-04
7.48974E-04	4.73121E-04	7.48974E-04	8.60167E-04	4.66410E-04	4.66410E-04
1.55116E-04	7.75581E-05	3.52385E-04	4.66409E-04	7.72028E-05	1.61236E-04
3.52385E-04	7.75581E-05	1.55116E-04	4.66409E-04	1.61236E-04	7.72028E-05

$$b_{3d2z^2-x^2-y^2}(\vec{k}, \vec{r}) = \frac{1}{\sqrt{N}} \sum_{\vec{R}_v} e^{i\vec{k} \cdot \vec{R}_v} \phi_{3d2z^2-x^2-y^2}(\vec{r} - \vec{R}_v), \quad (3-15)$$

$$b_{3dx^2-y^2}(\vec{k}, \vec{r}) = \frac{1}{\sqrt{N}} \sum_{\vec{R}_v} e^{i\vec{k} \cdot \vec{R}_v} \phi_{3dx^2-y^2}(\vec{r} - \vec{R}_v). \quad (3-16)$$

For future references in Chapter IV and V, notations $b_1(\vec{k}, \vec{r})$, $b_2(\vec{k}, \vec{r})$, $b_3(\vec{k}, \vec{r})$, $b_4(\vec{k}, \vec{r})$, and $b_5(\vec{k}, \vec{r})$ are also equivalently used for the Bloch sums given in Eqs. (3-12), (3-13), (3-14), (3-15), and (3-16) respectively.

The 3d atomic wave functions $\phi_{3dxy}(\vec{r})$, $\phi_{3dyz}(\vec{r})$, $\phi_{3dzx}(\vec{r})$, $\phi_{3d2z^2-x^2-y^2}(\vec{r})$, and $\phi_{3dx^2-y^2}(\vec{r})$ are each expressed in terms of a set of Gaussian type orbitals (GTO's). The details will be given in Chapter V. The radial wave function of the 3d orbital is generated in tabular form, using Clementi's Tables of Atomic Wave Functions⁽¹⁹⁾. The tabulated values of the radial wave function, $\phi_{3d}(r)$, are then curve fitted in terms of Gaussians in the following fashion

$$\phi_{3d}(r) = \sum_{i=1}^{i_m} \alpha_i r^2 e^{-\zeta_i r}, \quad (3-17)$$

where $i_m = 7$ is the number of α_i 's and ζ_i 's needed to obtain a reasonably accurate fit of $\phi_{3d}(r)$.

The values of α_i 's and ζ_i 's determined through the curve-fitting process are listed in Table VI.

A comparison of the fit with the tabulated 3d radial wave function is given in Table VII.

TABLE VI

PARAMETERS DETERMINED FROM CURVE-FITTING PROCESS FOR THE

$$3d \text{ RADIAL WAVE FUNCTION } \phi_{3d}(r) = \sum_{i=1}^m \alpha_i r^2 e^{-\zeta_i r^2}$$

i	α_i	ζ_i
1	2.74704E-03	1.26850E-01
2	4.63482E-02	2.82629E-01
3	4.18604E-01	7.16191E-01
4	2.70233E-00	1.79829E-00
5	1.20821E-01	4.55734E-00
6	3.45857E-01	1.21353E-01
7	7.06682E-01	4.01764E-01

TABLE VII

COMPARISON OF TABULAR AND CURVE FIT OF THE 3d RADIAL

$$\text{WAVE FUNCTION } \phi_{3d}(r) = \sum_{i=1}^{i_m} \alpha_i r^2 e^{-\zeta_i r^2}$$

r	Tabular	Curve Fit
0.0	0.0	0.0
0.28817E-02	0.54329E-05	0.28831E-05
0.57634E-02	0.42370E-04	0.23049E-04
0.86450E-02	0.13941E-03	0.77699E-04
0.11527E-01	0.32221E-03	0.18390E-03
0.14408E-01	0.61364E-03	0.35838E-03
0.17290E-01	0.10340E-02	0.61777E-03
0.20172E-01	0.16014E-02	0.97814E-03
0.23053E-01	0.23315E-02	0.14550E-02
0.25935E-01	0.32381E-02	0.20637E-02
0.28817E-01	0.43330E-02	0.28188E-02
0.34580E-01	0.71268E-02	0.48223E-02
0.40343E-01	0.10776E-01	0.75680E-02
0.46107E-01	0.15320E-01	0.11146E-01
0.51870E-01	0.20784E-01	0.15630E-01
0.57634E-01	0.27172E-01	0.21080E-01
0.63397E-01	0.34481E-01	0.27540E-01
0.69160E-01	0.42693E-01	0.35037E-01
0.74924E-01	0.51784E-01	0.43585E-01
0.80687E-01	0.61722E-01	0.53176E-01
0.86450E-01	0.72470E-01	0.63792E-01
0.97977E-01	0.96227E-01	0.87961E-01
0.10950E 00	0.12269E 00	0.11568E 00
0.12103E 00	0.15147E 00	0.14641E 00
0.13256E 00	0.18218E 00	0.17950E 00
0.14408E 00	0.21443E 00	0.21425E 00
0.15561E 00	0.24785E 00	0.25005E 00
0.16714E 00	0.28212E 00	0.28628E 00
0.17866E 00	0.31691E 00	0.32241E 00
0.19019E 00	0.35193E 00	0.35812E 00
0.20172E 00	0.38695E 00	0.39310E 00
0.22477E 00	0.45607E 00	0.46031E 00
0.24782E 00	0.52278E 00	0.52370E 00
0.27088E 00	0.58599E 00	0.58366E 00
0.29393E 00	0.64496E 00	0.64053E 00
0.31698E 00	0.69917E 00	0.69437E 00
0.34004E 00	0.74837E 00	0.74476E 00
0.36309E 00	0.79244E 00	0.79094E 00
0.38614E 00	0.83141E 00	0.83221E 00
0.40920E 00	0.86539E 00	0.86805E 00
0.43225E 00	0.89459E 00	0.89822E 00
0.47836E 00	0.93959E 00	0.94248E 00

TABLE VII (Continued)

r	Tabular	Curve Fit
0.52447E 00	0.96867E 00	0.96881E 00
0.57057E 00	0.98425E 00	0.98211E 00
0.61668E 00	0.98868E 00	0.98606E 00
0.66279E 00	0.98413E 00	0.98262E 00
0.70889E 00	0.97248E 00	0.97270E 00
0.75500E 00	0.95536E 00	0.95690E 00
0.80111E 00	0.93414E 00	0.93601E 00
0.84721E 00	0.90993E 00	0.91118E 00
0.89332E 00	0.88362E 00	0.88370E 00
0.98553E 00	0.82744E 00	0.82546E 00
0.10777E 01	0.76971E 00	0.76781E 00
0.11700E 01	0.71287E 00	0.71258E 00
0.12622E 01	0.65834E 00	0.65961E 00
0.13544E 01	0.60686E 00	0.60850E 00
0.14466E 01	0.55877E 00	0.55966E 00
0.15388E 01	0.51419E 00	0.51391E 00
0.16310E 01	0.47304E 00	0.47192E 00
0.17232E 01	0.43519E 00	0.43391E 00
0.18155E 01	0.40045E 00	0.39958E 00
0.19999E 01	0.33940E 00	0.34010E 00
0.21843E 01	0.28810E 00	0.28946E 00
0.23687E 01	0.24489E 00	0.24560E 00
0.25532E 01	0.20832E 00	0.20796E 00
0.27376E 01	0.17722E 00	0.17629E 00
0.29220E 01	0.15065E 00	0.14983E 00
0.31064E 01	0.12786E 00	0.12758E 00
0.32909E 01	0.10828E 00	0.10856E 00
0.34753E 01	0.91437E-01	0.92046E-01
0.36597E 01	0.76964E-01	0.77595E-01
0.40286E 01	0.53940E-01	0.54027E-01
0.43974E 01	0.37230E-01	0.36809E-01
0.47663E 01	0.25308E-01	0.24840E-01
0.51351E 01	0.16955E-01	0.16756E-01
0.55040E 01	0.11207E-01	0.11295E-01
0.58729E 01	0.73172E-02	0.75516E-02
0.62417E 01	0.47243E-02	0.49562E-02
0.66106E 01	0.30196E-02	0.31635E-02
0.69794E 01	0.19125E-02	0.19519E-02

CHAPTER IV

THE SECULAR EQUATION

Employing the set of Bloch tight-binding bases $b_1(\vec{k}, \vec{r})$, $b_2(\vec{k}, \vec{r})$, $b_3(\vec{k}, \vec{r})$, $b_4(\vec{k}, \vec{r})$, and $b_5(\vec{k}, \vec{r})$ as described in Chapter III, the trial wave function for the 3d bands at any point in the Brillouin zone can be approximated by

$$\Psi_\lambda(\vec{k}, \vec{r}) = \sum_{i=1}^5 a_\lambda^i b_i(\vec{k}, \vec{r}), \quad (4-1)$$

where the subscript λ designates the transformation properties under the operations of the group of the wave vector, and where a_λ^i 's are determined mainly by symmetry.

Using the one-electron Hamiltonian shown below

$$H = -\frac{1}{2} \nabla^2 + V(\vec{r}) \quad (4-2)$$

the Schrödinger equation can be written as

$$[H - E_\lambda(k)] \Psi_\lambda(\vec{k}, \vec{r}) = 0 \quad (4-3)$$

Multiplying both sides of Eq. (4-3) by $b_\nu^*(\vec{k}, \vec{r})$ and integrating over \vec{r} yields the five equations.

$$\sum_{\beta=1}^5 a_\lambda^\beta(\vec{k}) [H_{1,\beta}(\vec{k}) - E_\lambda(\vec{k}) S_{1,\beta}(\vec{k})] = 0, \quad (4-4)$$

$$\sum_{\beta=1}^5 a_\lambda^\beta(\vec{k}) [H_{2,\beta}(\vec{k}) - E_\lambda(\vec{k}) S_{2,\beta}(\vec{k})] = 0, \quad (4-5)$$

$$\sum_{\beta=1}^5 a_{\lambda}^{\beta}(\vec{k}) [H_{3,\beta}(\vec{k}) - E_{\lambda}(\vec{k}) S_{3,\beta}(\vec{k})] = 0, \quad (4-6)$$

$$\sum_{\beta=1}^5 a_{\lambda}^{\beta}(\vec{k}) [H_{4,\beta}(\vec{k}) - E_{\lambda}(\vec{k}) S_{4,\beta}(\vec{k})] = 0, \quad (4-7)$$

$$\sum_{\beta=1}^5 a_{\lambda}^{\beta}(\vec{k}) [H_{5,\beta}(\vec{k}) - E_{\lambda}(\vec{k}) S_{5,\beta}(\vec{k})] = 0. \quad (4-8)$$

where $H_{\alpha,\beta}(\vec{k})$ and $S_{\alpha,\beta}(\vec{k})$ with α running from 1 through 5 are defined as the following integrals

$$H_{\alpha,\beta}(\vec{k}) = \int b_{\alpha}^*(\vec{k}, \vec{r}) H b_{\beta}(\vec{k}, \vec{r}) d\tau, \quad (4-9)$$

$$S_{\alpha,\beta}(\vec{k}) = \int b_{\alpha}^*(\vec{k}, \vec{r}) b_{\beta}(\vec{k}, \vec{r}) d\tau. \quad (4-10)$$

The condition for these five equations to possess a non-trivial solution leads to the following secular equation.

$$\det |H_{\alpha,\beta}(\vec{k}) - E_{\lambda}(\vec{k}) S_{\alpha,\beta}(\vec{k})| = 0 \quad (4-11)$$

For each value of \vec{k} , the solution of this equation will yield five allowed values for the energy $E_{\lambda i}(\vec{k})$ where the roots are arranged in increasing order in magnitude

$$E_{\lambda 1}(\vec{k}) \leq E_{\lambda 2}(\vec{k}) \leq E_{\lambda 3}(\vec{k}) \leq E_{\lambda 4}(\vec{k}) \leq E_{\lambda 5}(\vec{k})$$

At points of high symmetry in the Brillouin zone, some of the $E_{\lambda i}(\vec{k})$ will be degenerated.

Evaluation of the matrix elements $H_{\alpha,\beta}(\vec{k})$ and $S_{\alpha,\beta}(\vec{k})$ must first be carried out in order to determine the roots of the secular equation.

Using the Bloch sum as given in Eq. (3-1), $H_{\alpha,\beta}(\vec{k})$ can be written as

$$H_{\alpha,\beta}(\vec{k}) = \frac{1}{N} \sum_{\vec{R}_\nu} \sum_{\vec{R}_\nu} e^{i\vec{k}\cdot(\vec{R}_\nu - \vec{R}_\nu)} \int \phi_\alpha^*(\vec{r} - \vec{R}_\nu) H \phi_\beta(\vec{r} - \vec{R}_\nu) dR. \quad (4-12)$$

For each value of \vec{R}_ν , the summation over \vec{R}_ν yields the same result, since the operator H is invariant under any symmetry translation. As the number of lattice sites in the crystal is represented schematically by N , the matrix element $H_{\alpha,\beta}(\vec{k})$ reduces to

$$H_{\alpha,\beta}(\vec{k}) = \sum_{\vec{R}_\nu} e^{i\vec{k}\cdot\vec{R}_\nu} \int \phi_\alpha^*(\vec{r}) H \phi_\beta(\vec{r} - \vec{R}_\nu) d\tau,$$

which can be rewritten in simpler notations as

$$H_{\alpha,\beta}(\vec{k}) = \sum_{\vec{R}_\nu} e^{i\vec{k}\cdot\vec{R}_\nu} \langle \phi_\alpha(\vec{0}) | H | \phi_\beta(\vec{R}_\nu) \rangle. \quad (4-13)$$

A similar reduction carried out for $S_{\alpha,\beta}(\vec{k})$ yields

$$\begin{aligned} S_{\alpha,\beta}(\vec{k}) &= \sum_{\vec{R}_\nu} e^{i\vec{k}\cdot\vec{R}_\nu} \int \phi_\alpha^*(\vec{r}) \phi_\beta(\vec{r} - \vec{R}_\nu) d\tau \\ &= \sum_{\vec{R}_\nu} e^{i\vec{k}\cdot\vec{R}_\nu} \langle \phi_\alpha(\vec{0}) | \phi_\beta(\vec{R}_\nu) \rangle \end{aligned} \quad (4-14)$$

It is clear that each matrix element is reduced to a sum over the crystal lattice of a number of multi-center integrals. It is also clear that the integrand in each matrix element involves a product of an orbital centered about the origin, an orbital centered about a lattice site \vec{R}_ν and, perhaps, some third function involving the crystal potential centered about a third lattice site, hence the term multi-center integral. Using the one electron Hamiltonian H as given in Eq. (4-2), the basic multi-center integrals become

$$\langle \phi_{\alpha}(\vec{0}) | \phi_{\beta}(\vec{R}_{\nu}) \rangle = \int \phi_{\alpha}^{*}(\vec{r}) \phi_{\beta}(\vec{r}-\vec{R}_{\nu}) d\tau, \quad (4-15)$$

$$\langle \phi_{\alpha}(\vec{0}) | -\frac{1}{2} \nabla^2 | \phi_{\beta}(\vec{R}_{\nu}) \rangle = \int \phi_{\alpha}^{*}(\vec{r}) (-\frac{1}{2} \nabla^2) \phi_{\beta}(\vec{r}-\vec{R}_{\nu}) d\tau, \quad (4-16)$$

$$\langle \phi_{\alpha}(\vec{0}) | V_{\text{crys}}(\vec{r}) | \phi_{\beta}(\vec{R}_{\nu}) \rangle = \int \phi_{\alpha}^{*}(\vec{r}) V_{\text{crys}}(\vec{r}) \phi_{\beta}(\vec{r}-\vec{R}_{\nu}) d\tau, \quad (4-17)$$

The integrals in Eqs. (4-15), (4-16) and (4-17) are respectively called overlap, kinetic energy, and potential energy integrals. Since these multicenter integrals are independent of the choice of \vec{k} , they need only to be calculated once for each crystal. The matrix elements of the secular equation for any given point in the Brillouin zone can then be evaluated by carrying out the appropriate sums over the crystal lattice after all the necessary multi-center integrals have been calculated. Thus the energies and wave functions associated with any given point in the Brillouin zone can be readily determined.

CHAPTER V

CALCULATION OF MULTICENTER INTEGRALS

A. Gaussian Orbitals

As mentioned in Chapter IV, the tight-binding matrix elements can be expressed in terms of a number of multicenter integrals of overlap, kinetic energy, and potential energy. Many well developed methods of high efficiency for evaluating overlap, and kinetic energy integrals can be found in the literature^(25,26,27). However, the same cannot be said about the potential energy integrals. Indeed, it is the difficulty of obtaining these potential energy integrals that has in the past imposed the very drastic approximations in the application of the tight-binding method. The most frequently used assumptions come under the name of the nearest-neighbor approximation. In this approximation one assumes that all potential energy integrals in which the two orbitals are separated by more than a primitive lattice vector, \vec{a}_j , are negligible, and further that in evaluating these integrals the only three-center integrals to be considered are those in which the third center coincides with one of the atomic orbitals or lies in an adjacent cell.

In order to avoid such approximations in the present investigation, a new procedure involving use of Gaussian-type orbitals (GTO's), discussed below, is employed to evaluate the potential energy integrals. GTO's are also used to evaluate the overlap and kinetic energy integrals. This new procedure proves to be so efficient that none of the assumption

involved in the nearest-neighbor approximation are necessary.

The definitions of the unnormalized Gaussian-type orbitals centered at \vec{A} are given below

$$\psi_{1s}^G(\alpha_i, \vec{r}_A) \equiv e^{-\alpha_i r_A^2},$$

$$\psi_{2p_x}^G(\alpha_i, \vec{r}_A) \equiv x_A e^{-\alpha_i r_A^2},$$

$$\psi_{2p_y}^G(\alpha_i, \vec{r}_A) \equiv y_A e^{-\alpha_i r_A^2},$$

$$\psi_{2p_z}^G(\alpha_i, \vec{r}_A) \equiv z_A e^{-\alpha_i r_A^2},$$

$$\psi_{3s}^G(\alpha_i, \vec{r}_A) \equiv r_A^2 e^{-\alpha_i r_A^2},$$

$$\psi_{3d_{xy}}^G(\alpha_i, \vec{r}_A) \equiv x_A y_A e^{-\alpha_i r_A^2},$$

$$\psi_{3d_{yz}}^G(\alpha_i, \vec{r}_A) \equiv y_A z_A e^{-\alpha_i r_A^2},$$

$$\psi_{3d_{zx}}^G(\alpha_i, \vec{r}_A) \equiv z_A x_A e^{-\alpha_i r_A^2},$$

$$\psi_{3d_{x^2}}^G(\alpha_i, \vec{r}_A) \equiv x_A^2 e^{-\alpha_i r_A^2},$$

$$\psi_{3d_{y^2}}^G(\alpha_i, \vec{r}_A) \equiv y_A^2 e^{-\alpha_i r_A^2},$$

and

$$\psi_{3d_{z^2}}^G(\alpha_i, \vec{r}_A) \equiv z_A^2 e^{-\alpha_i r_A^2},$$

where \vec{r}_A is a position vector referred to \vec{A} , x_A , y_A , and z_A are Cartesian coordinates of \vec{r}_A , and where the five spherical harmonics for $l = 2$ can

be constructed from appropriate linear combinations of ψ_{3dxy}^G , ψ_{3dyz}^G , ψ_{3dzx}^G , ψ_{3dx}^G , ψ_{3dy}^G , and ψ_{3dz}^G .

The Gaussian-type orbitals have an important and unique feature (26) in that the product of two Gaussians having their centers respectively at points \vec{A} and \vec{B} is, except for a constant factor K , itself a Gaussian with a center at a point \vec{D} , somewhere on the line joining the two points \vec{A} and \vec{B} , i.e., one can write the following equation,

$$\exp(-\alpha_1 r_A^2) \exp(-\alpha_2 r_B^2) = K \exp[-(\alpha_1 + \alpha_2) r_D^2] \quad (5-1)$$

where

$$K = \exp\left[-\left(\frac{\alpha_1 \alpha_2}{\alpha_1 + \alpha_2}\right) AB^2\right],$$

and where

$$AB^2 = |\vec{B} - \vec{A}|^2,$$

$$r_D^2 = |\vec{r} - \vec{D}|^2,$$

and

$$D_i = \frac{\alpha_1 A_i + \alpha_2 B_i}{\alpha_1 + \alpha_2}, \quad i = x, y, z.$$

The above mentioned feature of GTO's is used throughout in the formulations of the potential energy, kinetic energy, and overlap integrals described in the following sections.

B. Potential Energy Integrals

To evaluate the following potential energy integrals

$$\int \psi_i^G(\alpha_1, \vec{r}_A) V(\vec{r}) \psi_j^G(\alpha_2, \vec{r}_B) d\tau \equiv \langle \psi_i^G(\alpha_1, \vec{A}) | V | \psi_j^G(\alpha_2, \vec{B}) \rangle, \quad (5-2)$$

involving two unnormalized GTO's, $\psi_i^G(\alpha_1, \vec{r}_A)$ and $\psi_j^G(\alpha_2, \vec{r}_B)$, with i and j representing the various orbital indices, $1s$, $2p_x$, $2p_y$, $2p_z$, $3s$, $3d_{xy}$, $3d_{yz}$, $3d_{zx}$, $3d_x^2$, $3d_y^2$, and $3d_z^2$, centered at \vec{A} and \vec{B} , one uses a Fourier expansion for $V(\vec{r})$ as given in Eq. (2-9),

$$V(\vec{r}) = \sum_{\vec{K}_V} V(\vec{K}_V) \cos \vec{K}_V \cdot \vec{r}_C. \quad (2-9)$$

The summation is over all reciprocal lattice vectors. $V(\vec{K}_V)$ are the tabulated Fourier coefficients evaluated according to Eq. (2-43), and \vec{r}_C is a position vector referring to \vec{C} as its origin. See Figure 3. The point \vec{C} may be chosen to be any atomic site.

Using the Fourier expansion of $V(\vec{r})$, the potential energy integrals become

$$\langle \psi_i^G(\alpha_1, \vec{r}_A) | V | \psi_j^G(\alpha_2, \vec{r}_B) \rangle = \sum_{\vec{K}_V} V(\vec{K}_V) \langle \psi_i^G(\alpha_1, \vec{r}_A) | \cos \vec{K}_V \cdot \vec{r}_C | \psi_j^G(\alpha_2, \vec{r}_B) \rangle. \quad (5-3)$$

The Cartesian components for the position vector \vec{r}_A defined by $\vec{r}_A \equiv \vec{r} - \vec{A}$, see Fig. 3, are given by $x_A = X - A_x$, $y_A = Y - A_y$, and $z_A = Z - A_z$, where A_x , A_y , and A_z are Cartesian components of \vec{A} , with similar expressions for points \vec{B} , \vec{C} , and \vec{D} .

As will be shown later, all necessary potential energy, kinetic energy, and overlap integrals involving orbitals higher than the $1s$ orbital can be obtained by carrying out the appropriate differentiations and summations of the following basic integral involving only the $1s$ orbitals

$$\int e^{-\alpha_1 r_A^2} \cos \vec{K}_V \cdot \vec{r}_C e^{-\alpha_2 r_B^2} d\tau \equiv \langle \psi_{1s}^G(\alpha_1, \vec{r}_A) | \cos \vec{K}_V \cdot \vec{r}_C | \psi_{1s}^G(\alpha_2, \vec{r}_B) \rangle. \quad (5-4)$$

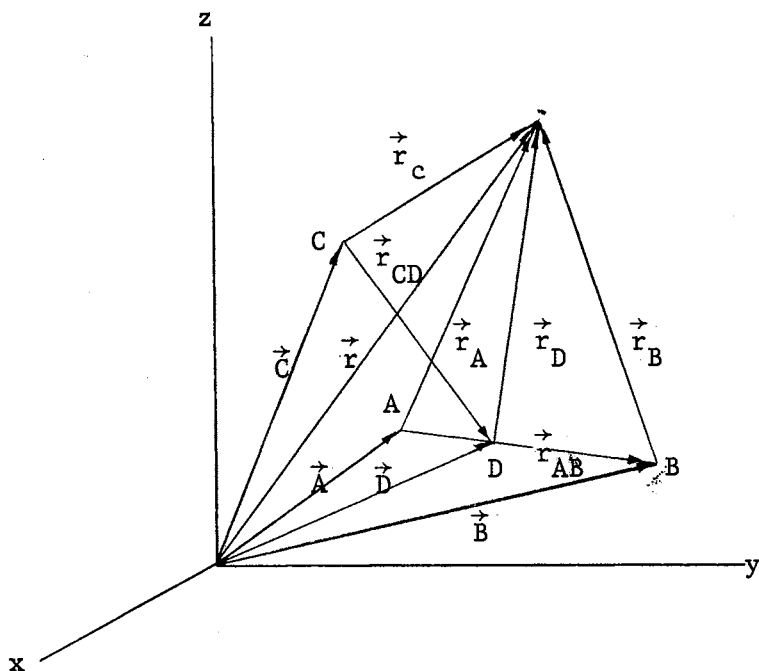


Figure 3. Relations Between Various Vectors in the Reduction of the Gaussian Orbitals

The result of the above integral can be put into a closed form and is given by

$$\langle \psi_{1s}^G(\alpha_1, \vec{r}_A) | \cos \vec{K}_v \cdot \vec{r}_c | \psi_{1s}^G(\alpha_2, \vec{r}_B) \rangle = \left(\frac{\pi}{\alpha_1 + \alpha_2} \right)^{3/2} e^{-\frac{1}{4} \frac{K_v^2}{\alpha_1 + \alpha_2}} e^{-\frac{\alpha_1 \alpha_2}{\alpha_1 + \alpha_2} \frac{AB^2}{\cos \vec{K}_v \cdot \vec{r}_{CD}}} \quad (5-5)$$

where $K_v^2 = \vec{K}_v \cdot \vec{K}_v$, and where $\vec{r}_{CD} = \vec{r}_{CB} - \vec{r}_{DB}$, See Figure 3. It can also be seen from Figure 3 that $\vec{r}_{DB} = \vec{B} - \vec{D}$, thus \vec{r}_{DB} is given by

$$\vec{r}_{DB} = \frac{\alpha_1}{\alpha_1 + \alpha_2} \vec{r}_{AB} \quad (5-6)$$

Using Eq. (5-6), and defining $U = \frac{\alpha_1}{\alpha_1 + \alpha_2}$ one can write

$$\vec{r}_{CD} = \vec{r}_{CB} - U \vec{r}_{AB}. \quad (5-7)$$

The following notations are defined to simplify the final expressions of the integrals.

$$H \equiv \frac{\alpha_1 \alpha_2}{\alpha_1 + \alpha_2},$$

$$Q \equiv \frac{1}{4} \frac{K_v^2}{\alpha_1 + \alpha_2},$$

$$K_x \equiv (\vec{K}_v)_x,$$

$$K_y \equiv (\vec{K}_v)_y,$$

$$K_z \equiv (\vec{K}_v)_z.$$

Using the simpler notation $1s(\alpha_1, \vec{A})$ for $\psi_{1s}^G(\alpha_1, \vec{r}_A)$, with the corresponding simpler notations for higher orbitals, and the notations defined above, the potential energy integral given by Eq. (5-6) can be written

$$\langle 1s(\alpha_1, \vec{A}) | \cos \vec{K}_v \cdot \vec{r}_c | 1s(\alpha_2, \vec{B}) \rangle = \left(\frac{\pi}{\alpha_1 + \alpha_2} \right)^{\frac{3}{2}} e^{-HAB^2} e^{-Q} \cos \vec{K}_v \cdot \vec{r}_{CD}. \quad (5-8)$$

All other potential energy integrals involving orbitals higher than the $1s$ orbital can be derived by appropriate differentiations and summations from Eq. (5-8). A number of examples are given below to show how this technique is used. For instance, the integral $\langle 1s(\alpha_1, \vec{r}_A) | \cos \vec{K}_v \cdot \vec{r}_c | 2p_x(\alpha_2, \vec{r}_B) \rangle$ can be obtained through the following differentiation.

$$\begin{aligned}
& \langle 1s(\alpha_1, \vec{r}_A) | \cos \vec{K}_v \cdot \vec{r}_c | 2p_x(\alpha_2, \vec{r}_B) \rangle \\
& \qquad \qquad \qquad (5-9) \\
& = \frac{1}{2\alpha_2} \frac{\partial}{\partial \vec{B}_x} \langle 1s(\alpha_1, \vec{r}_A) | \cos \vec{K}_v \cdot \vec{r}_c | 1s(\alpha_2, \vec{r}_B) \rangle .
\end{aligned}$$

By using the result given in Eq. (5-8) for $\langle 1s(\alpha_1, \vec{r}_A) | \cos \vec{K}_v \cdot \vec{r}_c | 1s(\alpha_2, \vec{r}_B) \rangle$ and performing the differentiation the final expression of the integral of Eq. (5-9) is found to be

$$\begin{aligned}
& \langle 1s(\alpha_1, \vec{r}_A) | \cos \vec{K}_v \cdot \vec{r}_c | 2p_x(\alpha_2, \vec{r}_B) \rangle \\
& = - \left(\frac{\pi}{\alpha_1 + \alpha_2} \right)^{\frac{3}{2}} e^{-HAB^2} e^{-Q} \left[\frac{\alpha_1}{\alpha_1 + \alpha_2} \overline{AB}_x \cos \vec{K}_v \cdot \vec{r}_{CD} \right. \\
& \quad \left. + \frac{K_x}{2(\alpha_1 + \alpha_2)} \sin \vec{K}_v \cdot \vec{r}_{CD} \right] .
\end{aligned}$$

The integrals $\langle 1s(\alpha_1, \vec{r}_A) | \cos \vec{K}_v \cdot \vec{r}_c | 2p_y(\alpha_2, \vec{r}_B) \rangle$ and $\langle 1s(\alpha_1, \vec{r}_A) | \cos \vec{K}_v \cdot \vec{r}_c | 2p_z(\alpha_2, \vec{r}_B) \rangle$ can be derived from the above integral by replacing the subscript x of \overline{AB}_x and K_x with those of y and z respectively. The integral $\langle 1s(\alpha_1, \vec{r}_A) | \cos \vec{K}_v \cdot \vec{r}_c | 2p_y(\alpha_2, \vec{r}_B) \rangle$ is, for example, given by

$$\begin{aligned}
& \langle 1s(\alpha_1, \vec{r}_A) | \cos \vec{K}_v \cdot \vec{r}_c | 2p_y(\alpha_2, \vec{r}_B) \rangle \\
& = - \left(\frac{\pi}{\alpha_1 + \alpha_2} \right)^{\frac{3}{2}} e^{-HAB^2} e^{-Q} \left[\frac{\alpha_1}{\alpha_1 + \alpha_2} \overline{AB}_y \cos \vec{K}_v \cdot \vec{r}_{CD} \right. \\
& \quad \left. + \frac{K_y}{2(\alpha_1 + \alpha_2)} \sin \vec{K}_v \cdot \vec{r}_{CD} \right] .
\end{aligned}$$

To evaluate the integral $\langle 1s(\alpha_2, \vec{A}) | \cos \vec{k}_v \cdot \vec{r}_c | 1s(\alpha_1, \vec{B}) \rangle$ one only needs to exchange α_1 and α_2 in the expression (5-10). This leads to the following integral

$$\langle 1s(\alpha_2, \vec{A}) | \cos \vec{k}_v \cdot \vec{r}_c | 1s(\alpha_1, \vec{B}) \rangle = \left(\frac{\pi}{\alpha_1 + \alpha_2} \right)^{\frac{3}{2}} e^{-HAB^2} e^{-Q} \cos \vec{k}_v \cdot \vec{r}_{CD'} ,$$

where

$$\vec{r}_{CD'} = \vec{r}_{CB} - \frac{\alpha_2}{\alpha_1 + \alpha_2} \vec{r}_{AB} .$$

Recalling the definition of U , one can write

$$\vec{r}_{CD'} = \vec{r}_{CB} - (1-U) \vec{r}_{AB} = \vec{r}_{CA} + U \vec{r}_{AB} .$$

If the point \vec{C} is chosen to be at an atomic site, then

$$\cos \vec{k}_v \cdot \vec{r}_{CD'} = \cos \vec{k}_v \cdot \vec{r}_{CD} .$$

The above method can be applied in general to obtain the integral

$$\langle \psi_i^G(\alpha_2, \vec{r}_A) | \cos \vec{k}_v \cdot \vec{r}_c | \psi_j^G(\alpha_1, \vec{r}_B) \rangle \text{ from } \langle \psi_i^G(\alpha_1, \vec{r}_A) | \cos \vec{k}_v \cdot \vec{r}_c | \psi_j^G(\alpha_2, \vec{r}_B) \rangle .$$

The following formulations, and a number of integrals, given by Eq. (5-24) through Eq. (5-30) need to be carried out before proceeding to obtain the potential energy integrals involving the lower orbitals and the 3d orbitals, $\langle 3dx^2(\alpha_1, \vec{A}) |$, $\langle 3dy^2(\alpha_1, \vec{A}) |$, and $\langle 3dz^2(\alpha_1, \vec{A}) |$.

$$\text{Since } \frac{\partial}{\partial Ax} \langle 2p_x(\alpha_1, \vec{A}) | = 2\alpha_1 X_A^2 e^{-\alpha_1 r_A^2} - e^{-\alpha_1 r_A^2}$$

$$\text{and } X_A^2 e^{-\alpha_1 r_A^2} = \frac{1}{2\alpha_1} \left[\frac{\partial}{\partial Ax} \langle 2p_x(\alpha_1, \vec{A}) | + \langle 1s(\alpha_1, \vec{A}) | \right] ,$$

$$\text{thus } \langle 3dx^2(\alpha_1, \vec{A}) | = \frac{1}{2\alpha_1} \left[\frac{\partial}{\partial Ax} \langle 2p_x(\alpha_1, \vec{A}) | + \langle 1s(\alpha_1, \vec{A}) | \right]. \quad (5-10)$$

A similar expression for $|3dx^2(\alpha_2, \vec{B})\rangle$ in terms of the lower orbitals is given below.

$$|3dx^2(\alpha_2, \vec{B})\rangle = \frac{1}{2\alpha_2} \left[\frac{\partial}{\partial Bx} |2p_x(\alpha_2, \vec{B})\rangle + |1s(\alpha_2, \vec{B})\rangle \right]. \quad (5-11)$$

The following definitions are useful.

$$\langle 3x^2(\alpha_1, \vec{A}) | \equiv \frac{1}{2\alpha_1} \frac{\partial}{\partial Ax} \langle 2p_x(\alpha_1, \vec{A}) |, \quad (5-12)$$

$$\langle 3y^2(\alpha_1, \vec{A}) | \equiv \frac{1}{2\alpha_1} \frac{\partial}{\partial Ay} \langle 2p_y(\alpha_1, \vec{A}) |, \quad (5-13)$$

$$\langle 3z^2(\alpha_1, \vec{A}) | \equiv \frac{1}{2\alpha_1} \frac{\partial}{\partial Az} \langle 2p_z(\alpha_1, \vec{A}) |, \quad (5-14)$$

$$|3x^2(\alpha_2, \vec{B})\rangle \equiv \frac{1}{2\alpha_2} \frac{\partial}{\partial Bx} |2p_x(\alpha_2, \vec{B})\rangle, \quad (5-15)$$

$$|3y^2(\alpha_2, \vec{B})\rangle \equiv \frac{1}{2\alpha_2} \frac{\partial}{\partial By} |2p_y(\alpha_2, \vec{B})\rangle, \quad (5-16)$$

$$|3z^2(\alpha_2, \vec{B})\rangle \equiv \frac{1}{2\alpha_2} \frac{\partial}{\partial Bz} |2p_z(\alpha_2, \vec{B})\rangle. \quad (5-17)$$

Following Eq. (5-10), and using Eq. (5-12) through Eq. (5-17) one can write down the following expressions.

$$\langle 3dx^2(\alpha_1, \vec{A}) | = \langle 3x^2(\alpha_1, \vec{A}) | + \frac{1}{2\alpha_1} \langle 1s(\alpha_1, \vec{A}) |, \quad (5-18)$$

$$\langle 3dy^2(\alpha_1, \vec{A}) | = \langle 3y^2(\alpha_1, \vec{A}) | + \frac{1}{2\alpha_1} \langle 1s(\alpha_1, \vec{A}) |, \quad (5-19)$$

$$\langle 3dz^2(\alpha_1, \vec{A}) | = \langle 3z^2(\alpha_1, \vec{A}) | + \frac{1}{2\alpha_1} \langle 1s(\alpha_1, \vec{A}) | , \quad (5-20)$$

$$| 3dx^2(\alpha_2, \vec{B}) \rangle = | 3x^2(\alpha_2, \vec{B}) \rangle + \frac{1}{2\alpha_2} | 1s(\alpha_2, \vec{B}) \rangle , \quad (5-21)$$

$$| 3dy^2(\alpha_2, \vec{B}) \rangle = | 3y^2(\alpha_2, \vec{B}) \rangle + \frac{1}{2\alpha_2} | 1s(\alpha_2, \vec{B}) \rangle , \quad (5-22)$$

$$| 3dz^2(\alpha_2, \vec{B}) \rangle = | 3z^2(\alpha_2, \vec{B}) \rangle + \frac{1}{2\alpha_2} | 1s(\alpha_2, \vec{B}) \rangle . \quad (5-23)$$

The following integrals are derived in order to obtain the potential energy integrals involving the $\psi_{3dx^2}^G$, $\psi_{3dy^2}^G$ orbitals and the lower ones.

$$\begin{aligned} & \langle 1s(\alpha_1, \vec{A}) | \cos \vec{K}_v \cdot \vec{r}_c | 3x^2(\alpha_2, \vec{B}) \rangle \\ &= \frac{1}{2\alpha_2} \frac{\partial}{\partial B_x} \langle 1s(\alpha_1, \vec{A}) | \cos \vec{K}_v \cdot \vec{r}_c | 2p_x(\alpha_2, \vec{B}) \rangle \\ &= \left(\frac{\pi}{\alpha_1 + \alpha_2} \right)^{\frac{3}{2}} e^{-\overline{HAB}^2} e^{-Q} \left\{ \frac{1}{(\alpha_1 + \alpha_2)} \left[\frac{\alpha_1}{\alpha_2} \left(\frac{\alpha_1 \alpha_2}{\alpha_1 + \alpha_2} \overline{AB}^2 - \frac{1}{2} \right) - \frac{K_x^2}{4(\alpha_1 + \alpha_2)} \right] \right. \\ & \quad \left. \cos \vec{K}_v \cdot \vec{r}_{CD} + \frac{\alpha_1}{(\alpha_1 + \alpha_2)} \overline{AB}_x K_x \sin \vec{K}_v \cdot \vec{r}_{CD} \right\} \end{aligned} \quad (5-24)$$

$$\begin{aligned} & \langle 2p_x(\alpha_1, \vec{A}) | \cos \vec{K}_v \cdot \vec{r}_c | 3x^2(\alpha_2, \vec{B}) \rangle \\ &= \frac{1}{2\alpha_2} \frac{\partial}{\partial B_x} \langle 2p_x(\alpha_1, \vec{A}) | \cos \vec{K}_v \cdot \vec{r}_c | 2p_x(\alpha_2, \vec{B}) \rangle \quad (5-25) \\ &= \left(\frac{\pi}{\alpha_1 + \alpha_2} \right)^{\frac{3}{2}} e^{-\overline{HAB}^2} \frac{e^{-Q}}{(\alpha_1 + \alpha_2)^2} \left\{ \left[\frac{\alpha_1^2 \alpha_2}{\alpha_1 + \alpha_2} \overline{AB}_x^3 - \frac{3}{2} \alpha_1 \overline{AB}_x + \frac{2\alpha_1 - \alpha_2}{4(\alpha_1 + \alpha_2)} \overline{AB}_x K_x^2 \right] \right. \\ & \quad \left. \cos \vec{K}_v \cdot \vec{r}_{CD} + \left[\frac{\alpha_1}{4\alpha_2} K_x - \frac{1}{2} K_x + \frac{\alpha_1(2\alpha_2 - \alpha_1)}{2(\alpha_1 + \alpha_2)} \overline{AB}_x^2 K_x + \frac{K_x^3}{8(\alpha_1 + \alpha_2)} \right] \sin \vec{K}_v \cdot \vec{r}_{CD} \right\}, \end{aligned}$$

$$\begin{aligned}
& \langle 2p_x(\alpha_1, \vec{A}) | \cos \vec{K}_v \cdot \vec{r}_c | 3y^2(\alpha_2, \vec{B}) \rangle \\
&= \frac{1}{2\alpha_2} \frac{\partial}{\partial B_y} \langle 2p_x(\alpha_1, \vec{A}) | \cos \vec{K}_v \cdot \vec{r}_c | 2p_y(\alpha_2, \vec{B}) \rangle \\
&= \left(\frac{\pi}{\alpha_1 + \alpha_2} \right)^{\frac{3}{2}} e^{-\overline{HAB}^2} \frac{e^{-Q}}{(\alpha_1 + \alpha_2)^2} \left\{ \left[\frac{\alpha_1^2 \alpha_2}{\alpha_1 + \alpha_2} \overline{AB}_y^2 \overline{AB}_x - \frac{1}{2} \alpha_1 \overline{AB}_x + \frac{\alpha_1}{2(\alpha_1 + \alpha_2)} \overline{AB}_y K_x K_y \right. \right. \\
&\quad \left. \left. - \frac{\alpha_2}{4(\alpha_1 + \alpha_2)} \overline{AB}_x K_y^2 \right] \cos \vec{K}_v \cdot \vec{r}_{CD} + \left[\frac{\alpha_1}{4\alpha_2} K_x + \frac{\alpha_1 \alpha_2}{\alpha_1 + \alpha_2} \overline{AB}_x \overline{AB}_y K_y \right. \right. \\
&\quad \left. \left. - \frac{\alpha_1^2}{2(\alpha_1 + \alpha_2)} \overline{AB}_y^2 K_x + \frac{K_y^2 K_x}{8(\alpha_1 + \alpha_2)} \right] \sin \vec{K}_v \cdot \vec{r}_{CD} \right\}, \tag{5-26}
\end{aligned}$$

$$\begin{aligned}
& \langle 3dxy(\alpha_1, \vec{A}) | \cos \vec{K}_v \cdot \vec{r}_c | 3x^2(\alpha_2, \vec{B}) \rangle \\
&= \frac{1}{2\alpha_1} \frac{\partial}{\partial A_y} \langle 2p_x(\alpha_1, \vec{A}) | \cos \vec{K}_v \cdot \vec{r}_c | 3x^2(\alpha_2, \vec{B}) \rangle \\
&= \left(\frac{\pi}{\alpha_1 + \alpha_2} \right)^{\frac{3}{2}} e^{-\overline{HAB}^2} e^{-Q} \frac{1}{(\alpha_1 + \alpha_2)^3} \left\{ \left[\frac{1}{8\alpha_2} (\alpha_1 - 2\alpha_2) K_x K_y + \alpha_1 \alpha_2 \overline{AB}_x \overline{AB}_y (\overline{HAB}_x^2 - \frac{3}{2}) \right. \right. \\
&\quad \left. \left. + \frac{1}{4(\alpha_1 + \alpha_2)} ((2\alpha_1 \alpha_2 - \alpha_2^2) \overline{AB}_x \overline{AB}_y K_x^2 \right. \right. \\
&\quad \left. \left. + (2\alpha_1 \alpha_2 - \alpha_1^2) \overline{AB}_x^2 K_x K_y + \frac{1}{4} K_x^3 K_y \right] \right. \\
&\quad \left. \cos \vec{K}_v \cdot \vec{r}_{CD} + \left[\frac{1}{2} (2\alpha_2 - \alpha_1) (\overline{HAB}_x^2 - \frac{1}{2}) \overline{AB}_y \right. \right. \\
&\quad \left. \left. K_x - \frac{1}{2} \alpha_1 (\overline{HAB}_x^2 - \frac{3}{2}) \overline{AB}_x K_y \right. \right. \\
&\quad \left. \left. + \frac{1}{8(\alpha_1 + \alpha_2)} (\alpha_2 \overline{AB}_y K_x^3 + (\alpha_2 - 2\alpha_1) \overline{AB}_x \right. \right. \\
&\quad \left. \left. K_x^2 K_y \right] \sin \vec{K}_v \cdot \vec{r}_{CD} \right\}, \tag{5-27}
\end{aligned}$$

$$\begin{aligned}
& \langle 3dxy(\alpha_1, \vec{A}) | \cos \vec{k}_v \cdot \vec{r}_c | 3z^2(\alpha_2, \vec{B}) \rangle \\
&= \frac{1}{2\alpha_1} \frac{\partial}{\partial A_y} \langle 2p_x(\alpha_1, \vec{A}) | \cos \vec{k}_v \cdot \vec{r}_c | 3z^2(\alpha_2, \vec{B}) \rangle \\
&= \left(\frac{\pi}{\alpha_1 + \alpha_2}\right)^{\frac{3}{2}} e^{-HAB^2} e^{-Q} \frac{1}{(\alpha_1 + \alpha_2)^2} \left\{ \left[H(\overline{HAB}_z^2 - \frac{1}{2}) \overline{AB}_x \overline{AB}_z + \frac{1}{2(\alpha_1 + \alpha_2)} \right. \right. \\
&\quad \left. \left. (\overline{HAB}_z (\overline{AB}_x K_z K_y + \overline{AB}_y K_x K_z) + \frac{\alpha_1}{4\alpha_2} K_x K_y) \right. \right. \\
&\quad \left. \left. - \frac{1}{4(\alpha_1 + \alpha_2)^2} (\alpha_2^2 \overline{AB}_y \overline{AB}_x K_z^2 + \alpha_1^2 \overline{AB}_z^2 \right. \right. \\
&\quad \left. \left. K_x K_y - \frac{1}{4} K_z^2 K_x K_y) \right] \cos \vec{k}_v \cdot \vec{r}_{CD} \right. \\
&\quad \left. + \left[\frac{1}{2(\alpha_1 + \alpha_2)} (2\alpha_2 \overline{HAB}_z \overline{AB}_x \overline{AB}_y K_z - \alpha_1 \right. \right. \\
&\quad \left. \left. (\overline{HAB}_z^2 - \frac{1}{2}) (\overline{AB}_x K_y + \overline{AB}_y K_x) \right) \right. \right. \\
&\quad \left. \left. + \frac{1}{4(\alpha_1 + \alpha_2)^2} (-\alpha_1 \overline{AB}_z K_z K_y K_x + \frac{1}{2} \alpha_2 \right. \right. \\
&\quad \left. \left. (\overline{AB}_y K_z^2 K_x + \overline{AB}_x K_z^2 K_y) \right] \sin \vec{k}_v \cdot \vec{r}_{CD} \right\}, (5-28)
\end{aligned}$$

$$\begin{aligned}
& \langle 3x^2(\alpha_1, \vec{A}) | \cos \vec{k}_v \cdot \vec{r}_c | 3y^2(\alpha_2, \vec{B}) \rangle \\
&= \frac{1}{2\alpha_1} \frac{\partial}{\partial A_x} \langle 2p_x(\alpha_1, \vec{A}) | \cos \vec{k}_v \cdot \vec{r}_c | 3y^2(\alpha_2, \vec{B}) \rangle \\
&= \left(\frac{\pi}{\alpha_1 + \alpha_2}\right)^{\frac{3}{2}} e^{-HAB^2} e^{-Q} \frac{1}{(\alpha_1 + \alpha_2)^2} \left\{ \left[(\overline{HAB}^2 - \frac{1}{2}) (\overline{HAB}_y^2 - \frac{1}{2}) + \frac{(\alpha_1^2 K_x^2 + \alpha_2^2 K_y^2)}{8\alpha_1 \alpha_2 (\alpha_1 + \alpha_2)} \right. \right.
\end{aligned}$$

$$\begin{aligned}
& - \frac{(\alpha_1 \overline{AB}^2 \overline{K_x^2} + \alpha_2 \overline{AB}^2 \overline{K_y^2})}{4(\alpha_1 + \alpha_2)^2} + \frac{\overline{HAB} \overline{AB}}{(\alpha_1 + \alpha_2)} \overline{K_x K_y} \\
& + \frac{\overline{K_x^2} \overline{K_y^2}}{16(\alpha_1 + \alpha_2)^2} \cos \vec{K}_v \cdot \vec{r}_{CD} \\
& + \left[\frac{-\alpha_1 (\overline{HAB}^2 \overline{K_x^2} - \frac{1}{2} \overline{AB} \overline{K_x^2})}{(\alpha_1 + \alpha_2)} + \frac{\alpha_2 (\overline{HAB}^2 \overline{K_x^2} - \frac{1}{2} \overline{AB} \overline{K_x^2})}{(\alpha_1 + \alpha_2)} \right. \\
& \left. - \frac{(\alpha_1 \overline{AB} \overline{K_x^2} \overline{K_z^2} - \alpha_2 \overline{AB} \overline{K_x^2} \overline{K_y^2})}{4(\alpha_1 + \alpha_2)^2} \right] \sin \vec{K}_v \cdot \vec{r}_{CD} \}.
\end{aligned} \tag{5-29}$$

Now, by using the results in Eq. (5-21), the integral

$\langle 1s(\alpha_1, \vec{r}_A) | \cos \vec{K}_v \cdot \vec{r}_c | 3dx^2(\alpha_2, \vec{r}_B) \rangle$ can finally be given by

$$\begin{aligned}
& \langle 1s(\alpha_1, \vec{r}_A) | \cos \vec{K}_v \cdot \vec{r}_c | 3dx^2(\alpha_2, \vec{r}_B) \rangle \\
& = \frac{1}{2\alpha_2} \langle 1s(\alpha_1, \vec{r}_A) | \cos \vec{K}_v \cdot \vec{r}_c | 1s(\alpha_2, \vec{r}_B) \rangle + \langle 1s(\alpha_1, \vec{r}_A) | \cos \vec{K}_v \cdot \vec{r}_c | 3x^2(\alpha_2, \vec{r}_B) \rangle.
\end{aligned} \tag{5-30}$$

In addition to Eqs. (5-9) and (5-30) the process of using the differentiation technique to obtain thirteen more integrals, from which all other potential energy integrals needed in this calculation can be derived, are given below to illustrate in more detail on how this technique is used.

$$\begin{aligned}
& \langle 1s(\alpha_1, \vec{r}_A) | \cos \vec{K}_v \cdot \vec{r}_c | 3dxy(\alpha_2, \vec{r}_B) \rangle \\
& = \frac{1}{2\alpha_2} \frac{\partial}{\partial B_y} \langle 1s(\alpha_1, \vec{r}_A) | \cos \vec{K}_v \cdot \vec{r}_c | 2p_x(\alpha_2, \vec{r}_B) \rangle,
\end{aligned} \tag{5-31}$$

$$\begin{aligned}
& \langle 2p_x(\alpha_1, \vec{r}_A) | \cos \vec{K}_v \cdot \vec{r}_c | 2p_x(\alpha_2, \vec{r}_B) \rangle \\
&= \frac{1}{2\alpha_1} \frac{\partial}{\partial A_x} \langle 1s(\alpha_1, \vec{r}_A) | \cos \vec{K}_v \cdot \vec{r}_c | 2p_x(\alpha_2, \vec{r}_B) \rangle, \quad (5-32)
\end{aligned}$$

$$\begin{aligned}
& \langle 2p_x(\alpha_1, \vec{r}_A) | \cos \vec{K}_v \cdot \vec{r}_c | 2p_y(\alpha_2, \vec{r}_B) \rangle \\
&= \frac{1}{2\alpha_1} \frac{\partial}{\partial A_x} \langle 1s(\alpha_1, \vec{r}_A) | \cos \vec{K}_v \cdot \vec{r}_c | 2p_y(\alpha_2, \vec{r}_B) \rangle, \quad (5-33)
\end{aligned}$$

$$\begin{aligned}
& \langle 2p_x(\alpha_1, \vec{r}_A) | \cos \vec{K}_v \cdot \vec{r}_c | 3dxy(\alpha_2, \vec{r}_B) \rangle \\
&= \frac{1}{2\alpha_2} \frac{\partial}{\partial B_y} \langle 2p_x(\alpha_1, \vec{r}_A) | \cos \vec{K}_v \cdot \vec{r}_c | 2p_x(\alpha_2, \vec{r}_B) \rangle, \quad (5-34)
\end{aligned}$$

$$\begin{aligned}
& \langle 2p_x(\alpha_1, \vec{r}_A) | \cos \vec{K}_v \cdot \vec{r}_c | 3dyz(\alpha_2, \vec{r}_B) \rangle \\
&= \frac{1}{2\alpha_2} \frac{\partial}{\partial B_z} \langle 2p_x(\alpha_1, \vec{r}_A) | \cos \vec{K}_v \cdot \vec{r}_c | 2p_y(\alpha_2, \vec{r}_B) \rangle. \quad (5-35)
\end{aligned}$$

$$\begin{aligned}
& \langle 2p_x(\alpha_1, \vec{r}_A) | \cos \vec{K}_v \cdot \vec{r}_c | 3dx^2(\alpha_2, \vec{r}_B) \rangle \\
&= \frac{1}{2\alpha_2} \langle 2p_x(\alpha_1, \vec{r}_A) | \cos \vec{K}_v \cdot \vec{r}_c | 1s(\alpha_2, \vec{r}_B) \rangle + \langle 2p_x(\alpha_1, \vec{r}_A) | \cos \vec{K}_v \cdot \vec{r}_c | \\
& \quad 3x^2(\alpha_2, \vec{r}_B) \rangle, \quad (5-36)
\end{aligned}$$

$$\begin{aligned}
& \langle 2p_x(\alpha_1, \vec{r}_A) | \cos \vec{K}_v \cdot \vec{r}_c | 3dy^2(\alpha_2, \vec{r}_B) \rangle \\
&= \frac{1}{2\alpha_2} \langle 2p_x(\alpha_1, \vec{r}_A) | \cos \vec{K}_v \cdot \vec{r}_c | 1s(\alpha_2, \vec{r}_B) \rangle + \langle 2p_x(\alpha_1, \vec{r}_A) | \cos \vec{K}_v \cdot \vec{r}_c | \\
& \quad 3dy^2(\alpha_2, \vec{r}_B) \rangle, \quad (5-37)
\end{aligned}$$

$$\begin{aligned}
& \langle 3dx^2(\alpha_1, \vec{r}_A) | \cos \vec{K}_v \cdot \vec{r}_c | 3dy^2(\alpha_2, \vec{r}_B) \rangle \\
&= \langle 3x^2(\alpha_1, \vec{r}_A) | \cos \vec{K}_v \cdot \vec{r}_c | 3y^2(\alpha_2, \vec{r}_B) \rangle + \frac{1}{2\alpha_1} \langle 1s(\alpha_1, \vec{r}_A) | \cos \vec{K}_v \cdot \vec{r}_c | \\
&\qquad\qquad\qquad 3y^2(\alpha_2, \vec{r}_B) \rangle \\
&+ \frac{1}{2\alpha_2} \langle 3x^2(\alpha_1, \vec{r}_A) | \cos \vec{K}_v \cdot \vec{r}_c | 1s(\alpha_2, \vec{r}_B) \rangle + \frac{1}{4\alpha_1\alpha_2} \langle 1s(\alpha_1, \vec{r}_A) | \cos \vec{K}_v \cdot \vec{r}_c | \\
&\qquad\qquad\qquad 1s(\alpha_2, \vec{r}_B) \rangle . \qquad (5-43)
\end{aligned}$$

By carrying out the differentiations outlined above, the closed form expressions of sixteen basic potential energy integrals are obtained and listed in Table VIII. Any other necessary potential energy integrals not listed in the table can be obtained readily from one of the sixteen integrals. For instance to obtain an expression for the integral

$$\langle \psi_j^G(\alpha_1, \vec{r}_A) | \cos \vec{K}_v \cdot \vec{r}_c | \psi_i^G(\alpha_2, \vec{r}_B) \rangle \quad \text{from} \quad \langle \psi_i^G(\alpha_1, \vec{r}_A) | \cos \vec{K}_v \cdot \vec{r}_c | \psi_j^G(\alpha_2, \vec{r}_B) \rangle$$

one only needs to change the components of the vector \vec{AB} to its negative values, and exchange α_1 and α_2 . As an example, the integral

$$\langle 2p_x(\alpha_1, \vec{r}_A) | \cos \vec{K}_v \cdot \vec{r}_c | 1s(\alpha_2, \vec{r}_B) \rangle$$

can be readily obtained from Table VIII and the result is found to be

$$\begin{aligned}
& \langle 2p_x(\alpha_1, \vec{r}_A) | \cos \vec{K}_v \cdot \vec{r}_c | 1s(\alpha_2, \vec{r}_B) \rangle \\
&= \left(\frac{\pi}{\alpha_1 + \alpha_2} \right)^{\frac{3}{2}} e^{-\overline{HAB}^2} e^{-Q} \left[\frac{\alpha_2}{\alpha_1 + \alpha_2} \overline{AB}_x \cos \vec{K}_v \cdot \vec{r}_{CD} - \frac{K_x}{2(\alpha_1 + \alpha_2)} \sin \vec{K}_v \cdot \vec{r}_{CD} \right] .
\end{aligned}$$

C. Overlap Integrals

The overlap integrals, $\langle \psi_i^G(\alpha_1, \vec{r}_A) | \psi_j^G(\alpha_2, \vec{r}_B) \rangle$, involving two un-

TABLE VIII

THE POTENTIAL ENERGY INTEGRALS ARE GIVEN IN THE FOLLOWING FORM $\langle \psi_1^G(\alpha_1, \vec{r}_A) | \cos \vec{k}_v \cdot \vec{r}_c | \psi_j^G(\alpha_2, \vec{r}_B) \rangle$

$$= C_1 [f(\alpha_1, \alpha_2, \overline{AB}, \vec{k}_v) \cos \vec{k}_v \cdot \vec{r}_{CD} + g(\alpha_1, \alpha_2, \overline{AB}, \vec{k}_v) \sin \vec{k}_v \cdot \vec{r}_{CD}], \text{ WHERE } C_1 = \left(\frac{\pi}{\alpha_1 + \alpha_2}\right)^{\frac{3}{2}} e^{-\overline{HAB}^2} e^{-Q}. \quad H$$

$$\text{AND } Q \text{ HAVE THE SAME MEANING AS THEY ARE DEFINED PREVIOUSLY, I.E., } H = \frac{\alpha_1 \alpha_2}{\alpha_1 + \alpha_2}, \text{ AND } Q = \frac{k_v^2}{4(\alpha_1 + \alpha_2)}.$$

Integrals	$f(\alpha_1, \alpha_2, \overline{AB}, \vec{k}_v)$	$g(\alpha_1, \alpha_2, \overline{AB}, \vec{k}_v)$
$\langle 1s(\alpha_1, \vec{r}_A) \cos \vec{k}_v \cdot \vec{r}_c 1s(\alpha_2, \vec{r}_B) \rangle$	1	0
$\langle 1s(\alpha_1, \vec{r}_A) \cos \vec{k}_v \cdot \vec{r}_c 2p_x(\alpha_2, \vec{r}_B) \rangle$	$-\frac{\alpha_1}{\alpha_1 + \alpha_2} \overline{AB}_x$	$-\frac{k_x}{2(\alpha_1 + \alpha_2)}$
$\langle 1s(\alpha_1, \vec{r}_A) \cos \vec{k}_v \cdot \vec{r}_c 3d_{xy}(\alpha_2, \vec{r}_B) \rangle$	$\frac{\alpha_1^2 \overline{AB}_y \overline{AB}_x - \frac{1}{4} k_x k_y}{(\alpha_1 + \alpha_2)^2}$	$\frac{\alpha_1 (\overline{AB}_y k_x + \overline{AB}_x k_y)}{2(\alpha_1 + \alpha_2)^2}$
$\langle 1s(\alpha_1, \vec{r}_A) \cos \vec{k}_v \cdot \vec{r}_c 3d_x^2(\alpha_2, \vec{r}_B) \rangle$	$\frac{1}{2\alpha_2} + \frac{\alpha_1 (\overline{HAB}_x^2 - \frac{1}{2})}{\alpha_2 (\alpha_1 + \alpha_2)} - \frac{k_x^2}{4(\alpha_1 + \alpha_2)^2}$	$\frac{\overline{HAB}_x k_x}{\alpha_2 (\alpha_1 + \alpha_2)^2}$
$\langle 2p_x(\alpha_1, \vec{r}_A) \cos \vec{k}_v \cdot \vec{r}_c 2p_x(\alpha_2, \vec{r}_B) \rangle$	$\frac{2(\alpha_1 + \alpha_2) - k_x^2 - 4\alpha_1 \alpha_2 \overline{AB}_x^2}{4(\alpha_1 + \alpha_2)^2}$	$-\frac{(\alpha_2 - \alpha_1) \overline{AB}_x k_x}{2(\alpha_1 + \alpha_2)^2}$
$\langle 2p_x(\alpha_1, \vec{r}_A) \cos \vec{k}_v \cdot \vec{r}_c 2p_y(\alpha_2, \vec{r}_B) \rangle$	$-\frac{k_x k_y + 4\alpha_1 \alpha_2 \overline{AB}_x \overline{AB}_y}{4(\alpha_1 + \alpha_2)^2}$	$\frac{\alpha_1 k_x \overline{AB}_y - \alpha_2 \overline{AB}_x k_y}{2(\alpha_1 + \alpha_2)^2}$

TABLE VIII (Continued)

Integrals	$f(\alpha_1, \alpha_2, \vec{AB}, \vec{k}_v)$	$g(\alpha_1, \alpha_2, \vec{AB}, \vec{k}_v)$
$\langle 2p_x(\alpha_1, \vec{r}_A) \cos \vec{k}_v \cdot \vec{r}_c 3d_{xy}(\alpha_2, \vec{r}_B) \rangle$	$-\frac{\alpha_1 (\frac{1}{2} - \overline{HAB}_x^2) \overline{AB}_y}{(\alpha_1 + \alpha_2)^2}$ $+ \frac{\alpha_1 \overline{AB}_y \overline{K}_x^2 + (\alpha_1 - \alpha_2) \overline{AB}_x \overline{K}_x \overline{K}_y}{4(\alpha_1 + \alpha_2)^3}$	$-\frac{(\frac{1}{2} - \overline{HAB}_x^2) \overline{K}_y}{2(\alpha_1 + \alpha_2)^2}$ $+ \frac{\frac{1}{4} \overline{K}_x^2 \overline{K}_y - \alpha_1 (\alpha_1 - \alpha_2) \overline{AB}_x \overline{AB}_y \overline{K}_x}{2(\alpha_1 + \alpha_2)^3}$
$\langle 2p_x(\alpha_1, \vec{r}_A) \cos \vec{k}_v \cdot \vec{r}_c 3d_{yz}(\alpha_2, \vec{r}_B) \rangle$	$\frac{\alpha_1 \overline{K}_x \overline{K}_y \overline{AB}_z + \alpha_1 \overline{K}_x \overline{K}_z \overline{AB}_y - \alpha_2 \overline{K}_x \overline{K}_z \overline{AB}_x}{4(\alpha_1 + \alpha_2)^3}$ $+ \frac{\alpha_1 \overline{HAB}_x \overline{AB}_y \overline{AB}_z}{(\alpha_1 + \alpha_2)^2}$	$\frac{H(\overline{AB}_x \overline{AB}_y \overline{K}_z + \overline{AB}_x \overline{AB}_z \overline{K}_y)}{2(\alpha_1 + \alpha_2)^2}$ $- \frac{\alpha_1^2 \overline{AB}_y \overline{AB}_z \overline{K}_x - \frac{1}{4} \overline{K}_x \overline{K}_y \overline{K}_z}{2(\alpha_1 + \alpha_2)^3}$
$\langle 2p_x(\alpha_1, \vec{r}_A) \cos \vec{k}_v \cdot \vec{r}_c 3d_x^2(\alpha_2, \vec{r}_B) \rangle$	$\frac{\overline{AB}_x}{2(\alpha_1 + \alpha_2)} + \frac{\alpha_1 \overline{AB}_x (\overline{HAB}_x^2 - \frac{3}{2})}{(\alpha_1 + \alpha_2)^2}$ $+ \frac{(2\alpha_1 - \alpha_2) \overline{AB}_x \overline{K}_x^2}{4(\alpha_1 + \alpha_2)^3}$	$-\frac{\overline{K}_x}{4\alpha_2(\alpha_1 + \alpha_2)} + \frac{(\alpha_1 - 2\alpha_2) \overline{K}_x}{4\alpha_2(\alpha_1 + \alpha_2)^2}$ $+ \frac{(2\alpha_1 \alpha_2 - \alpha_1^2) \overline{AB}_x^2 \overline{K}_x + \frac{1}{4} \overline{K}_y^3}{2(\alpha_1 + \alpha_2)^3}$
$\langle 2p_x(\alpha_1, \vec{r}_A) \cos \vec{k}_v \cdot \vec{r}_c 3d_y^2(\alpha_2, \vec{r}_B) \rangle$	$\frac{\overline{AB}_x}{2(\alpha_1 + \alpha_2)} + \frac{\alpha_1 \overline{AB}_x (\overline{HAB}_y^2 - \frac{1}{2})}{(\alpha_1 + \alpha_2)^2}$ $+ \frac{(2\alpha_1 \overline{AB}_y \overline{K}_x \overline{K}_y - \alpha_2 \overline{AB}_x \overline{K}_x^2)}{4(\alpha_1 + \alpha_2)^3}$	$-\frac{\overline{K}_x}{4(\alpha_1 + \alpha_2)^2}$ $+ \frac{\alpha_1 \overline{AB}_y (2\alpha_2 \overline{AB}_x \overline{K}_y - \alpha_1 \overline{AB}_y \overline{K}_x) + \frac{1}{4} \overline{K}_y^2 \overline{K}_x}{2(\alpha_1 + \alpha_2)^3}$

TABLE VIII (Continued)

Integrals	$f(\alpha_1, \alpha_2, \vec{AB}, \vec{K}_V)$	$g(\alpha_1, \alpha_2, \vec{AB}, \vec{K}_V)$
$\langle 3d_{xy}(\alpha_1, \vec{r}_A) \rangle$	$\frac{H\overline{AB} \overline{AB} (2H\overline{AB}^2 - 1)}{(\alpha_1 + \alpha_2)^2}$	$-\frac{\alpha_1 \overline{HAB} \overline{AB} (\overline{AB} \overline{K}_x + \overline{AB} \overline{K}_y) - \alpha_2 \overline{HAB} \overline{AB} (\overline{AB} \overline{K}_x + \overline{AB} \overline{K}_y)}{(\alpha_1 + \alpha_2)^3}$
$ \cos \vec{K}_V \cdot \vec{r}_C $	$\frac{(\alpha_2^2 \overline{AB} \overline{AB} \overline{K}_x \overline{K}_y + \alpha_1^2 \overline{AB} \overline{AB} \overline{K}_y \overline{K}_x - \frac{1}{4} \overline{K}_x \overline{K}_y^2 \overline{K}_z)}{2(\alpha_1 + \alpha_2)^4}$	$-\frac{(\alpha_2 \overline{AB} \overline{K}_x - \alpha_1 \overline{AB} \overline{K}_y)}{2(\alpha_1 + \alpha_2)^3}$
$3d_{yz}(\alpha_2, \vec{r}_B) \rangle$	$+\frac{H(\overline{AB} \overline{AB} \overline{K}_x^2 + \overline{AB} \overline{AB} \overline{K}_y^2 + \overline{AB} \overline{AB} \overline{K}_z^2 + \overline{AB}^2 \overline{K}_x \overline{K}_y) - \frac{1}{2} \overline{K}_x \overline{K}_y}{2(\alpha_1 + \alpha_2)^3}$	$-\frac{\alpha_1 \overline{AB} \overline{K}_x \overline{K}_y^2 - \alpha_2 \overline{AB} \overline{K}_y \overline{K}_x^2 + (\alpha_1 - \alpha_2) \overline{AB} \overline{K}_x \overline{K}_y \overline{K}_z}{4(\alpha_1 + \alpha_2)^4}$
$\langle 3d_{xy}(\alpha_1, \vec{r}_A) \rangle$	$\frac{\alpha_2^2 \overline{AB} \overline{AB} - \frac{1}{4} \overline{K}_x \overline{K}_y}{2\alpha_2(\alpha_1 + \alpha_2)^2}$	$-\frac{(\overline{AB} \overline{K}_x + \overline{AB} \overline{K}_y)}{2(\alpha_1 + \alpha_2)^2} + \frac{\alpha_2 \overline{AB} \overline{K}_x^3 + (\alpha_2 - 2\alpha_1) \overline{AB} \overline{K}_x^2 \overline{K}_y}{8(\alpha_1 + \alpha_2)^4}$
$ \cos \vec{K}_V \cdot \vec{r}_C $	$+\frac{\frac{1}{8\alpha_2} (\alpha_1 - 2\alpha_2) \overline{K}_x \overline{K}_y + \alpha_1 \alpha_2 \overline{AB} \overline{AB} (H\overline{AB}^2 - \frac{3}{2})}{(\alpha_1 + \alpha_2)^3}$	$+\frac{(\alpha_2 - \frac{1}{2}\alpha_1) (H\overline{AB}^2 - \frac{1}{2}) \overline{AB} \overline{K}_x - \frac{1}{2}\alpha_1 \overline{AB} \overline{K}_y (H\overline{AB}^2 - \frac{3}{2})}{(\alpha_1 + \alpha_2)^3}$
$3d_x^2(\alpha_2, \vec{r}_B) \rangle$	$+\frac{(2\alpha_1 \alpha_2 - \alpha_2^2) \overline{AB} \overline{AB} \overline{K}_x^2 + (2\alpha_1 \alpha_2 - \alpha_1^2) \overline{AB} \overline{AB} \overline{K}_y^2 + \frac{1}{4} \overline{K}_x^3 \overline{K}_y}{4(\alpha_1 + \alpha_2)^4}$	

TABLE VIII (Continued)

Integrals	$f(\alpha_1, \alpha_2, \vec{AB}, \vec{K}_V)$	$g(\alpha_1, \alpha_2, \vec{AB}, \vec{K}_V)$
$\langle 3d_{xy}(\alpha_1, \vec{r}_A) \rangle$	$\frac{\alpha_2^2 \overline{AB} \overline{AB} - \frac{1}{4} \overline{K} \overline{K}}{2\alpha_2(\alpha_1 + \alpha_2)^2}$	$-\frac{\overline{AB} \overline{K} + \overline{AB} \overline{K}}{2(\alpha_1 + \alpha_2)^2}$
$ \cos \vec{K}_V \cdot \vec{r}_C $	$-\frac{\alpha_2^2 \overline{AB} \overline{AB} \overline{K}^2 + \alpha_1^2 \overline{AB}^2 \overline{K} \overline{K} - \frac{1}{4} \overline{K}^2 \overline{K} \overline{K}}{4(\alpha_1 + \alpha_2)^4}$	$+\frac{-\alpha_1 \overline{AB} \overline{K} \overline{K} \overline{K} + \frac{1}{2} \alpha_2 (\overline{AB} \overline{K}^2 \overline{K} + \overline{AB} \overline{K}^2 \overline{K})}{4(\alpha_1 + \alpha_2)^4}$
$3d_z^2(\alpha_2, \vec{r}_B) \rangle$	$+\frac{H(\overline{HAB}_z^2 - \frac{1}{2}) \overline{AB} \overline{AB}}{(\alpha_1 + \alpha_2)^2} + \frac{H \overline{AB} (\overline{AB} \overline{K} \overline{K} + \overline{AB} \overline{K} \overline{K}) + \frac{\alpha_1}{4\alpha_2} \overline{K} \overline{K}}{2(\alpha_1 + \alpha_2)^3}$	$+\frac{2\alpha_2 \overline{HAB} \overline{AB} \overline{AB} \overline{K} - \alpha_1 (\overline{HAB}_z^2 - \frac{1}{2}) (\overline{AB} \overline{K} + \overline{AB} \overline{K})}{2(\alpha_1 + \alpha_2)^3}$
$\langle 3d_x^2(\alpha_1, \vec{r}_A) \rangle$	$\frac{\frac{3}{4} + \overline{HAB}_x^2 (\overline{HAB}_x^2 - 3)}{(\alpha_1 + \alpha_2)^2} - \frac{(\alpha_1^2 - 4\alpha_1\alpha_2 + \alpha_2^2) (1 - 2\overline{HAB}_x^2) \overline{K}_x^2}{8\alpha_1\alpha_2(\alpha_1 + \alpha_2)^3}$	
$ \cos \vec{K}_V \cdot \vec{r}_C $	$+\frac{\overline{K}_x^4}{16(\alpha_1 + \alpha_2)^2} + \frac{(\overline{HAB}_x^2 - \frac{1}{2})}{2\alpha_2(\alpha_1 + \alpha_2)} - \frac{\overline{K}_x^2}{8\alpha_1(\alpha_1 + \alpha_2)^2} + \frac{(\overline{HAB}_x^2 - \frac{1}{2})}{2\alpha_1(\alpha_1 + \alpha_2)}$	$\frac{(\alpha_1 - \alpha_2) (\frac{3}{2} - \overline{HAB}_x^2) \overline{AB} \overline{K}_x}{(\alpha_1 + \alpha_2)^3} + \frac{(\alpha_2 - \alpha_1) \overline{AB} \overline{K}_x^3}{4(\alpha_1 + \alpha_2)^4}$
$3d_x^2(\alpha_2, \vec{r}_B) \rangle$	$-\frac{\overline{K}_x^2}{8\alpha_2(\alpha_1 + \alpha_2)^2} + \frac{1}{4\alpha_1\alpha_2}$	

TABLE VIII (Continued)

Integrals	$f(\alpha_1, \alpha_2, \vec{AB}, \vec{K}_V)$	$g(\alpha_1, \alpha_2, \vec{AB}, \vec{K}_V)$
$\langle 3d_x^2(\alpha_1, \vec{r}_A) \rangle$	$\frac{(\overline{HAB}_x^2 - \frac{1}{2})(\overline{HAB}_y^2 - \frac{1}{2})}{(\alpha_1 + \alpha_2)^2} - \frac{(\alpha_1^2 K_x^2 + \alpha_2^2 K_y^2)}{8\alpha_1\alpha_2(\alpha_1 + \alpha_2)^3} - \frac{(\alpha_1^2 \overline{AB}_y^2 K_x^2 + \alpha_2^2 \overline{AB}_x^2 K_y^2)}{4(\alpha_1 + \alpha_2)^4}$	$-\frac{\alpha_1(\overline{HAB}_y^2 - \frac{1}{2})\overline{AB}_x K_x}{(\alpha_1 + \alpha_2)^3} + \frac{\alpha_2(\overline{HAB}_x^2 - \frac{1}{2})\overline{AB}_y K_y}{(\alpha_1 + \alpha_2)^3}$
$ \cos \vec{K}_V \cdot \vec{r}_C $	$+ \frac{\overline{HAB}_x \overline{AB}_y K_x K_y}{(\alpha_1 + \alpha_2)^3} + \frac{K_x^2 K_y^2}{16(\alpha_1 + \alpha_2)^4} + \frac{(\overline{HAB}_y^2 - \frac{1}{2})}{2\alpha_2(\alpha_1 + \alpha_2)} - \frac{K_y^2}{8\alpha_1(\alpha_1 + \alpha_2)^2}$	$- \frac{(\alpha_1 \overline{AB}_y K_x^2 K_y - \alpha_2 \overline{AB}_x K_x K_y^2)}{4(\alpha_1 + \alpha_2)^4} + \frac{\overline{HAB}_y K_y}{2\alpha_1\alpha_2(\alpha_1 + \alpha_2)}$
$3d_y^2(\alpha_2, \vec{r}_B) \rangle$	$+ \frac{(\overline{HAB}_x^2 - \frac{1}{2})}{2\alpha_1(\alpha_1 + \alpha_2)} - \frac{K_x^2}{8\alpha_2(\alpha_1 + \alpha_2)^2} + \frac{1}{4\alpha_1\alpha_2}$	$- \frac{\overline{HAB}_x K_x}{2\alpha_1\alpha_2(\alpha_1 + \alpha_2)}$
$\langle 3d_{xy}(\alpha_1, \vec{r}_A) \rangle$	$\frac{(\frac{1}{2} - \overline{HAB}_x^2)(\frac{1}{2} - \overline{HAB}_y^2)}{(\alpha_1 + \alpha_2)^2} + \frac{H(\overline{AB}_y^2 K_x^2 + \overline{AB}_x^2 K_y^2) - \frac{1}{2}(K_x^2 + K_y^2)}{4(\alpha_1 + \alpha_2)^3}$	$\frac{(\alpha_1 - \alpha_2)[(\frac{1}{2} - \overline{HAB}_x^2)\overline{AB}_y K_y + (\frac{1}{2} - \overline{HAB}_y^2)\overline{AB}_x K_x]}{2(\alpha_1 + \alpha_2)^3}$
$ \cos \vec{K}_V \cdot \vec{r}_C $	$+ \frac{\frac{1}{4} K_x^2 K_y^2 - (\alpha_1 - \alpha_2)^2 \overline{AB}_x \overline{AB}_y K_x K_y}{4(\alpha_1 + \alpha_2)^4}$	$- \frac{(\alpha_1 - \alpha_2)(\overline{AB}_y K_x^2 K_y + \overline{AB}_x K_x K_y^2)}{8(\alpha_1 + \alpha_2)^4}$
$3d_{xy}(\alpha_2, \vec{r}_B) \rangle$		

normalized 3d GTO's are obtained by setting \vec{K}_v equal to zero in the corresponding potential energy integrals, $\langle \psi_1^G(\alpha_1, \vec{r}_A) | \cos \vec{K}_v \cdot \vec{r}_c | \psi_j^G(\alpha_2, \vec{r}_B) \rangle$ and are readily obtained from Table VIII.

D. Kinetic Energy Integrals

To obtain the analytical expressions for the kinetic energy integrals $\langle \psi_1^G(\alpha_1, \vec{r}_A) | -\frac{1}{2} \nabla^2 | \psi_j^G(\alpha_2, \vec{r}_B) \rangle$ involving two unnormalized GTO's, one again starts by obtaining the kinetic energy integral involving two 1s GTO's. The kinetic energy integrals involving higher orbitals can then be derived from this basic integral by appropriate differentiations and summations.

To do this, examine the factor in the integrand

$$\nabla^2 \psi_j^G(\alpha_2, \vec{r}_B) = \left(\frac{\partial^2}{\partial x^2} + \frac{\partial^2}{\partial y^2} + \frac{\partial^2}{\partial z^2} \right) \psi_j^G(\alpha_2; x_B, y_B, z_B) \quad (5-44)$$

where

$$x_B = x - B_x, \quad y_B = y - B_y, \quad \text{and} \quad z_B = z - B_z.$$

The Laplacian is invariant under translation of the coordinate system and hence,

$$\nabla^2 \psi_j^G(\alpha_2, \vec{r}_B) = \left(\frac{\partial^2}{\partial x_B^2} + \frac{\partial^2}{\partial y_B^2} + \frac{\partial^2}{\partial z_B^2} \right) \psi_j^G(\alpha_2, \vec{r}_B).$$

Because of the symmetric relationship of x_B and B_x in $\psi_j^G(\alpha_2; x_B, y_B, z_B)$ one obtains the relation

$$\frac{\partial}{\partial B_x} \psi_j^G(\alpha_2, \vec{r}_B) = \frac{\partial}{\partial x_B} \psi_j^G(\alpha_2, \vec{r}_B) \frac{\partial x_B}{\partial B_x}$$

$$= -\frac{\partial}{\partial x_B} \psi_j^G(\alpha_2, \vec{r}_B),$$

and similar relations for $\frac{\partial}{\partial B_y} \psi_j^G(\alpha_2, \vec{r}_B)$ and $\frac{\partial}{\partial B_z} \psi_j^G(\alpha_2, \vec{r}_B)$. Hence,

$$\nabla^2 \psi_j^G(\alpha_2, \vec{r}_B) = \nabla_B^2 \psi_j^G(\alpha_2, \vec{r}_B), \quad (5-45)$$

where

$$\nabla_B^2 = \frac{\partial^2}{\partial B_x^2} + \frac{\partial^2}{\partial B_y^2} + \frac{\partial^2}{\partial B_z^2}.$$

The relation given in Eq. (5-45) enables one to write

$$\begin{aligned} & \langle \psi_{1s}^G(\alpha_1, \vec{r}_A) | -\frac{1}{2} \nabla^2 | \psi_{1s}^G(\alpha_2, \vec{r}_B) \rangle \\ &= -\frac{1}{2} \nabla_B^2 \langle \psi_{1s}^G(\alpha_1, \vec{r}_A) | \psi_{1s}^G(\alpha_2, \vec{r}_B) \rangle \end{aligned} \quad (5-46)$$

The overlap integral $\langle \psi_{1s}^G(\alpha_1, \vec{r}_A) | \psi_{1s}^G(\alpha_2, \vec{r}_B) \rangle$ can be obtained, as stated earlier, by setting $\vec{K}_v = 0$ in the potential energy integral

$\langle \psi_{1s}^G(\alpha_1, \vec{r}_A) | \cos \vec{K}_v \cdot \vec{r}_c | \psi_{1s}^G(\alpha_2, \vec{r}_B) \rangle$, and is found to be

$$\langle \psi_{1s}^G(\alpha_1, \vec{r}_A) | \psi_{1s}^G(\alpha_2, \vec{r}_B) \rangle = \left(\frac{\pi}{\alpha_1 + \alpha_2} \right)^{\frac{3}{2}} e^{-\overline{HAB}^2}. \quad (5-47)$$

Using Eq. (5-47) in Eq. (5-46) one obtains

$$\begin{aligned} & \langle \psi_{1s}^G(\alpha_1, \vec{r}_A) | -\frac{1}{2} \nabla^2 | \psi_{1s}^G(\alpha_2, \vec{r}_B) \rangle \\ &= -\frac{1}{2} \nabla_B^2 \left[\left(\frac{\pi}{\alpha_1 + \alpha_2} \right)^{\frac{3}{2}} e^{-\overline{HAB}^2} \right]. \end{aligned} \quad (5-48)$$

In spherical polar coordinates the above equation can be written

$$\begin{aligned}
& \langle \psi_{1s}^G(\alpha_1, \vec{r}_A) | -\frac{1}{2} \nabla^2 | \psi_{1s}^G(\alpha_2, \vec{r}_B) \rangle \\
&= -\frac{1}{2} \left(\frac{\pi}{\alpha_1 + \alpha_2} \right)^{\frac{3}{2}} \frac{1}{\overline{AB}^2} \frac{\partial}{\partial \overline{AB}} \left(\overline{AB}^2 \frac{\partial}{\partial \overline{AB}} e^{-\overline{HAB}^2} \right). \quad (5-49)
\end{aligned}$$

By carrying out the differentiation the above integral is found to be

$$\begin{aligned}
& \langle \psi_{1s}^G(\alpha_1, \vec{r}_A) | -\frac{1}{2} \nabla^2 | \psi_{1s}^G(\alpha_2, \vec{r}_B) \rangle \\
&= \left(\frac{\pi}{\alpha_1 + \alpha_2} \right)^{\frac{3}{2}} e^{-\overline{HAB}^2} \left[\frac{3\alpha_1\alpha_2}{\alpha_1 + \alpha_2} - \frac{2\alpha_1^2\alpha_2^2}{(\alpha_1 + \alpha_2)^2} \overline{AB}^2 \right]. \quad (5-50)
\end{aligned}$$

All other kinetic energy integrals can be derived from the above integral by performing the appropriate differentiations and summations in a manner similar to that of obtaining the potential energy integrals from the basic integral $\langle \psi_{1s}^G(\alpha_1, \vec{r}_A) | \cos \vec{K}_v \cdot \vec{r}_c | \psi_{1s}^G(\alpha_2, \vec{r}_B) \rangle$ as discussed in Section B. For instance, the integral $\langle \psi_{1s}^G(\alpha_1, \vec{r}_A) | -\frac{1}{2} \nabla^2 | \psi_{2p_x}^G(\alpha_2, \vec{r}_B) \rangle$ is obtained by the following process

$$\begin{aligned}
& \langle \psi_{1s}^G(\alpha_1, \vec{r}_A) | -\frac{1}{2} \nabla^2 | \psi_{2p_x}^G(\alpha_2, \vec{r}_B) \rangle \\
&= \frac{1}{2\alpha_2} \frac{\partial}{\partial B_x} \langle \psi_{1s}^G(\alpha_1, \vec{r}_A) | -\frac{1}{2} \nabla^2 | \psi_{1s}^G(\alpha_2, \vec{r}_B) \rangle.
\end{aligned}$$

The final expression of the above integral, after carrying out the differentiation, is found to be

$$\begin{aligned}
& \langle \psi_{1s}^G(\alpha_1, \vec{r}_A) | -\frac{1}{2} \nabla^2 | \psi_{2p_x}^G(\alpha_2, \vec{r}_B) \rangle \\
&= \left(\frac{\pi}{\alpha_1 + \alpha_2} \right)^{\frac{3}{2}} e^{-\overline{HAB}^2} \left[-\frac{5\alpha_1^2\alpha_2}{(\alpha_1 + \alpha_2)^2} + \frac{2\alpha_1^3\alpha_2^2}{(\alpha_1 + \alpha_2)^3} \overline{AB}^2 \right] \frac{1}{\overline{AB}_x}. \quad (5-51)
\end{aligned}$$

In addition to the integrals in Eq. (5-50) and (5-51) fourteen more kinetic energy integrals are obtained, in a similar way as one obtained the corresponding potential energy integrals as listed in Table VIII, and are listed in Table IX. Similar techniques as used in Section B can be utilized to derive any other necessary kinetic energy integral from one of the sixteen integrals listed in Table IX.

TABLE IX

THE KINETIC ENERGY INTEGRALS ARE GIVEN IN THE FOLLOWING FORM $\langle \psi_i^G(\alpha_1, \vec{r}_A) | -\frac{1}{2} \nabla^2 | \psi_j^G(\alpha_2, \vec{r}_B) \rangle$
 $= C_2 h(\alpha_1, \alpha_2, \vec{AB}, \vec{K}_v)$, WHERE $C_2 = \left(\frac{\pi}{\alpha_1 + \alpha_2}\right)^{\frac{3}{2}} e^{-H\overline{AB}^2}$. H IS DEFINED AS $H = \frac{\alpha_1 \alpha_2}{\alpha_1 + \alpha_2}$.

Integrals	$h(\alpha_1, \alpha_2, \vec{AB}, \vec{K}_v)$
$\langle 1s(\alpha_1, \vec{r}_A) -\frac{1}{2} \nabla^2 1s(\alpha_2, \vec{r}_B) \rangle$	$H(3-2 \overline{HAB}^2)$
$\langle 1s(\alpha_1, \vec{r}_A) -\frac{1}{2} \nabla^2 2p_x(\alpha_2, \vec{r}_B) \rangle$	$\frac{H^2}{\alpha_2} (2\overline{HAB}^2 - 5) \overline{AB}_x$
$\langle 1s(\alpha_1, \vec{r}_A) -\frac{1}{2} \nabla^2 3d_{xy}(\alpha_2, \vec{r}_B) \rangle$	$\frac{2H^3}{\alpha_2} (\overline{HAB}^2 - \frac{7}{2}) \overline{AB}_x \overline{AB}_y$
$\langle 1s(\alpha_1, \vec{r}_A) -\frac{1}{2} \nabla^2 3dx^2(\alpha_2, \vec{r}_B) \rangle$	$-\frac{2H^3}{\alpha_2} (\overline{HAB}^2 - \frac{7}{2}) \overline{AB}_x^2 + \frac{H^2}{\alpha_2} (\overline{HAB}^2 - \frac{5}{2}) + \frac{H}{2\alpha_2} (3-2 \overline{HAB}^2)$
$\langle 2p_x(\alpha_1, \vec{r}_A) -\frac{1}{2} \nabla^2 2p_x(\alpha_2, \vec{r}_B) \rangle$	$\frac{H}{(\alpha_1 + \alpha_2)} \left(\frac{5}{2} - 7\overline{HAB}_x^2 + 2H^2 \overline{AB}^2 \overline{AB}_x^2 - \overline{HAB}^2\right)$

TABLE IX (Continued)

Integrals	$h(\alpha_1, \alpha_2, \vec{AB}, \vec{K}_v)$
$\langle 2p_x(\alpha_1, \vec{r}_A) -\frac{1}{2} \nabla^2 2p_y(\alpha_2, \vec{r}_B) \rangle$	$\frac{H^2}{(\alpha_1 + \alpha_2)} (2H\overline{AB}^2 - 7) \overline{AB}_x \overline{AB}_y$
$\langle 2p_x(\alpha_1, \vec{r}_A) -\frac{1}{2} \nabla^2 3d_{xy}(\alpha_2, \vec{r}_B) \rangle$	$-\frac{H^3}{\alpha_1 \alpha_2} \left[\frac{7}{2} - H(9\overline{AB}_x^2 + \overline{AB}^2) - 2H^2 \overline{AB}_x^2 \overline{AB}_y^2 \right] \overline{AB}_y$
$\langle 2p_x(\alpha_1, \vec{r}_A) -\frac{1}{2} \nabla^2 3d_{yz}(\alpha_2, \vec{r}_B) \rangle$	$-\frac{2H^4}{\alpha_1 \alpha_2} (\overline{HAB}^2 - \frac{9}{2}) \overline{AB}_x \overline{AB}_y \overline{AB}_z$
$\langle 2p_x(\alpha_1, \vec{r}_A) -\frac{1}{2} \nabla^2 3dx^2(\alpha_2, \vec{r}_B) \rangle$	$\frac{H^3}{\alpha_1 \alpha_2} \left[-2\overline{HAB}_x^2 (\overline{HAB}^2 - \frac{9}{2}) + 3(\overline{HAB}^2 - \frac{7}{2}) \right] \overline{AB}_x - \frac{H^2}{2\alpha_1 \alpha_2} (2\overline{HAB}^2 - 5) \overline{AB}_x$
$\langle 2p_x(\alpha_1, \vec{r}_A) -\frac{1}{2} \nabla^2 3dy^2(\alpha_2, \vec{r}_B) \rangle$	$\frac{H^3}{\alpha_1 \alpha_2} \left[-2\overline{HAB}_y^2 (\overline{HAB}^2 - \frac{9}{2}) + (\overline{HAB}^2 - \frac{7}{2}) \right] \overline{AB}_x - \frac{H^2}{2\alpha_1 \alpha_2} (2\overline{HAB}^2 - 5) \overline{AB}_x$
$\langle 3d_{xy}(\alpha_1, \vec{r}_A) -\frac{1}{2} \nabla^2 3d_{xy}(\alpha_2, \vec{r}_B) \rangle$	$\frac{H^3}{\alpha_1 \alpha_2} \left[\frac{7}{4} + H(\overline{HAB}^2 - \frac{9}{2})(\overline{AB}_x^2 + \overline{AB}_y^2) - 2H^2 \overline{AB}_x^2 \overline{AB}_y^2 (\overline{HAB}^2 - \frac{11}{2}) - \frac{H}{2} \overline{AB}^2 \right]$

TABLE IX (Continued)

Integrals	$h(\alpha_1, \alpha_2, \vec{AB}, \vec{K}_v)$
$\langle 3d_{xy}(\alpha_1, \vec{r}_A) -\frac{1}{2} \nabla^2 3d_{yz}(\alpha_2, \vec{r}_B) \rangle$	$\frac{H^4}{\alpha_1 \alpha_2} \left[-\frac{9}{2} - 2\overline{HAB}_y^2 (\overline{HAB}^2 - \frac{11}{2}) + \overline{HAB}^2 \right] \overline{AB}_x \overline{AB}_z$
$\langle 3d_{xy}(\alpha_1, \vec{r}_A) -\frac{1}{2} \nabla^2 3dx^2(\alpha_2, \vec{r}_B) \rangle$	$\left\{ \frac{H^4}{\alpha_1 \alpha_2} \left[-2\overline{HAB}_x^2 (\overline{HAB}^2 - \frac{11}{2}) + 3(\overline{HAB}^2 - \frac{9}{2}) \right] + \frac{H^3}{2\alpha_1 \alpha_2} (-2\overline{HAB}^2 + 7) \right\} \overline{AB}_x \overline{AB}_y$
$\langle 3d_{xy}(\alpha_1, \vec{r}_A) -\frac{1}{2} \nabla^2 3dz^2(\alpha_2, \vec{r}_B) \rangle$	$\left\{ \frac{H^4}{\alpha_1 \alpha_2} \left[-2\overline{HAB}_z^2 (\overline{HAB}^2 - \frac{11}{2}) + (\overline{HAB}^2 - \frac{9}{2}) \right] + \frac{H^3}{2\alpha_1 \alpha_2} (-2\overline{HAB}^2 + 7) \right\} \overline{AB}_x \overline{AB}_y$
$\langle 3dx^2(\alpha_1, \vec{r}_A) -\frac{1}{2} \nabla^2 3dx^2(\alpha_2, \vec{r}_B) \rangle$	$\frac{H^3}{\alpha_1 \alpha_2} \left[-2 H^2 \overline{AB}_x^4 (\overline{HAB}^2 - \frac{11}{2}) + 3\overline{HAB}_x^2 (2\overline{HAB}^2 - 9) - \frac{3}{2} (\overline{HAB}^2 - \frac{7}{2}) \right]$ $+ \frac{H^2}{2\alpha_1 \alpha_2} \left[-2 \overline{HAB}_x^2 (\overline{HAB}^2 - \frac{7}{2}) + (\overline{HAB}^2 - \frac{5}{2}) \right] + \frac{H^2}{2\alpha_1 \alpha_2} \left[-2 \overline{HAB}_x^2 (\overline{HAB}^2 - \frac{7}{2}) \right]$ $+ (\overline{HAB}^2 - \frac{5}{2}) \left] + \frac{H}{4\alpha_1 \alpha_2} (3 - 2 \overline{HAB}^2)$

TABLE IX (Continued)

Integrals	$h(\alpha_1, \alpha_2, \vec{AB}, \vec{K}_v)$
$\langle 3d_x^2(\alpha_1, \vec{r}_A) -\frac{1}{2} \nabla^2 3dy^2(\alpha_2, \vec{r}_B) \rangle$	$\frac{H^3}{2\alpha_1\alpha_2} \left[-2 H^2 \overline{AB}_x^2 \overline{AB}_y^2 (\overline{HAB}^2 - \frac{11}{2}) + H(\overline{HAB}^2 - \frac{9}{2}) (\overline{AB}_x^2 + \overline{AB}_y^2) - \frac{1}{2}(\overline{HAB}^2 - \frac{7}{2}) \right]$ $+ \frac{H^2}{2\alpha_1\alpha_2} \left[-2 \overline{HAB}_y^2 (\overline{HAB}^2 - \frac{7}{2}) + (\overline{HAB}^2 - \frac{5}{2}) \right] + \frac{H^2}{2\alpha_1\alpha_2} \left[-2 \overline{HAB}_x^2 (\overline{HAB}^2 - \frac{7}{2}) \right.$ $\left. + (\overline{HAB}^2 - \frac{5}{2}) \right] + \frac{H}{4\alpha_1\alpha_2} (3 - 2 \overline{HAB}^2)$

CHAPTER VI

RESULTS AND DISCUSSIONS

The results of the calculation for the "3d bands" of copper using tight-binding method with GTO's are reported in this chapter. The values of $E(\vec{k})$ versus \vec{k} along $[1, 0, 0]$ direction in the Brillouin zone are tabulated in Table X. The band structure, $E(\vec{k})$ versus \vec{k} along the above mentioned direction is shown in Figure 4. Table XI gives the energy differences of states which indicate the relative positions and widths of the bands at the X point from this calculation along with the results from other investigators. The 3d band width, $E(X_5) - E(X_1)$, is calculated by Segall⁽⁸⁾ as 0.300 Ryd and by Snow⁽²⁸⁾ as 0.189 Ryd. compared to the value of 0.121 Ryd from this calculation. The energy difference of $E(X_5) - E(X_3)$ is calculated to be 0.212 Ryd by Burdick⁽⁵⁾ and 0.170 Ryd by Snow and Weber⁽²⁸⁾ in contrast to 0.107 Ryd found in the present calculation. It is noticed that the energy difference, $E(X_5) - E(X_1)$, of the present calculation is narrower than those from other works, and it is also interesting to note that the experimental value of $E(X_5) - E(X_1)$ found by Berglund and Spicer⁽²⁹⁾ to be 0.205 Ryd and that by Fadley and Shirley⁽³⁰⁾ to be 0.221 Ryd, both of which are smaller, see Table XI, than the results calculated by Segall and Burdick. In the present calculation the results at the Γ point are rigorous within the model although the core states are not included in the trial function. This is due to the fact that the core orbitals neglected

TABLE X

THE CALCULATED VALUES OF $E(\vec{k})$ VS. \vec{k} FOR THE 3d BANDS OF COPPER ALONG $[1,0,0]$ DIRECTIONS BY TIGHT-BINDING METHOD ARE TABULATED IN THIS TABLE. THE BSW SYMBOLS ARE USED. IR AT THE HEAD OF EACH COLUMN STANDS FOR IRREDUCIBLE REPRESENTATIONS. UNIT OF ENERGY E IS IN RYDBERGS.

BSW Label	$\frac{a_0}{2\pi} \vec{k}$	Band 1		Band 2		Band 3		Band 4		Band 5	
		IR	E	IR	E	IR	E	IR	E	IR	E
Γ^0	0,0,0	12	-0.489	12	-0.489	25'	-0.523	25'	-0.523	25'	-0.523
	0.1,0,0	2	-0.488	1	-0.490	5	-0.522	5	-0.522	2'	-0.524
Δ	0.2,0,0	2	-0.487	1	-0.494	5	-0.519	5	-0.519	2'	-0.528
	0.3,0,0	2	-0.485	1	-0.502	5	-0.514	5	-0.514	2'	-0.533
Δ	0.4,0,0	2	-0.482	5	-0.507	5	-0.507	1	-0.515	2'	-0.540
	0.5,0,0	2	-0.479	5	-0.498	5	-0.498	1	-0.531	2'	-0.548
Δ	0.6,0,0	2	-0.475	5	-0.489	5	-0.489	1	-0.548	2'	-0.555
	0.7,0,0	2	-0.472	5	-0.480	5	-0.480	2'	-0.562	1	-0.564
Δ	0.8,0,0	2	-0.470	5	-0.472	5	-0.472	2'	-0.570	1	-0.576
	0.9,0,0	5	-0.466	5	-0.466	2	-0.468	2'	-0.570	1	-0.584
X	1,0,0	5	-0.464	5	-0.464	2	-0.467	3	-0.572	1	-0.586

TABLE XI.

COMPARISON OF VARIOUS CALCULATED AND EXPERIMENTAL RESULTS (ENERGIES IN RYDBERG)

Calculated				Experimental	
Source	$E(\Gamma_{12}) - E(\Gamma'_{25})$	$E(X_5) - E(X_1)$	$E(X_5) - E(X_3)$	Source	$E(X_5) - E(X_1)$
Segall ^a	0.072	0.300	0.244	Spicer ^e	0.205
Burdick ^b	0.058	0.249	0.212	Shirley ^f	0.221
Snow ^c					
Slater = 1	0.045	0.189	0.170		
Slater = $\frac{5}{6}$	0.046	0.224	0.180		
Howarth ^d	0.040	-----	0.268		
Present Calculation	0.034	0.121	0.107		

- a. Reference 8
b. Reference 5
c. Reference 28
d. Reference 2
e. Reference 29
f. Reference 30

contain only s , p_x , p_y , and p_z orbitals and these orbitals can never reproduce the d state transformation properties represented by Γ_{12} and Γ'_{25} . Thus the Γ_{12} and Γ'_{25} states are automatically orthogonal to the core states. It is clearly shown in Table XI that the energy difference, $E(\Gamma_{12}) - E(\Gamma'_{25})$, of 0.034 Ryd of the present calculation agrees reasonably well with some of the other calculations, for instance, Howarth's⁽²⁾ 0.040 Ryd for $E(\Gamma_{12}) - E(\Gamma_{25})$, although the value is again smaller than those given by all other investigators. The omission of the core states will not have any effect on $E(X_5)$, $E(X_3)$ since the X_5 , X_3 , and X_2 states are all d states, which cannot mix with the core s , p_x , p_y , and p_z states. At the X_1 point there is a possibility of mixing s -like and d -like wave functions. However, if the overlaps between the d orbitals and the orbitals representing the core states are small, which is assumed, then the mixing of s and d wave functions at this point can be ignored. Thus, the results at X point also represent a near rigorous solution within the model. Examination of Figure 4 shows that the free electron-like s - p band that crosses the d bands as would normally be seen in the band structure of copper is missing, since the $4s$ and $4p$ states are not included in the trial wave function in the present calculation.

The narrow d bands found in this calculation help to strengthen the widely held belief that the $3d$ orbitals are tightly bound and do constitute the major contributors to the so-called "3- d band". It is pointed out that⁽³¹⁾ the calculations of the band structures for transition metals are complicated due to the presence of d electrons which occupy narrow energy bands lying in a broad s - p band. It is also pointed out by various authors^(15,24,32) that certain properties, for instance,

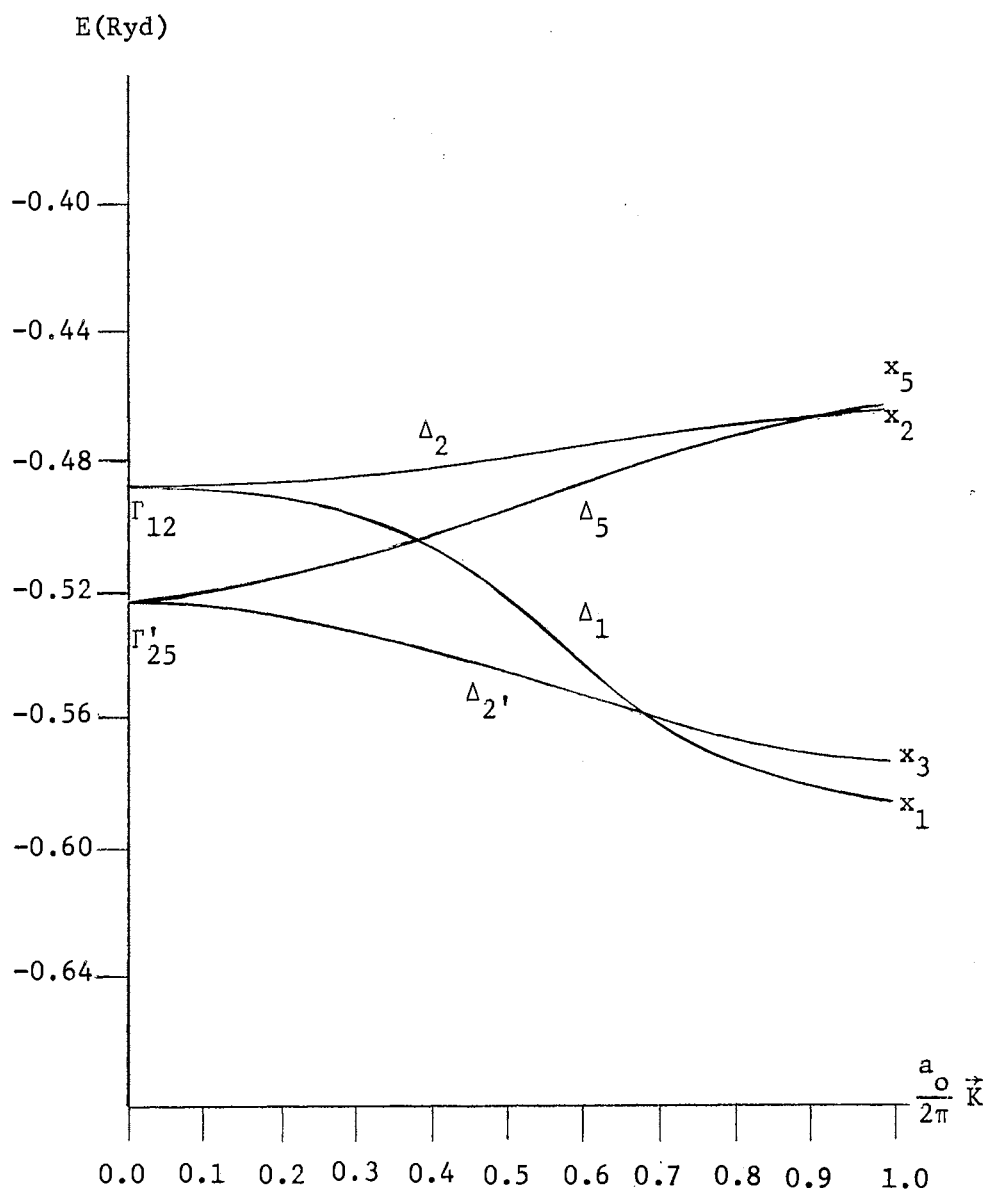


Figure 4. $E(\vec{k})$ Vs. \vec{k} Along $[1,0,0]$ Line

the band width and the relative positions of the band with respect to the Fermi energy, of the d bands are very sensitive to the crystal potential used in the calculation. The APW method suffers mainly from the inadequacy of the assumption of the muffin-tin type crystal potential in its calculation. It is known that⁽³³⁾, even in a self-consistent APW calculation, the muffin-tin type crystal potential casts some shadow on the certainty of the relative position of the d bands and leaves some doubt about the details of the Fermi surface of the material under study. This muffin-tin approximation is even more serious in the band structure calculations for transition-metal compounds⁽³⁴⁾. It is therefore felt that the difference in the crystal potential used in this calculation might also have contributed in some degree to the narrow bands reported here. Up to the present time no investigation on the structure of the d band of copper using the extended tight-binding method of Lafon and Lin with a non-muffin tin crystal potential has been reported. For copper, in which the d band is important, the present investigation appears to be the first try in this direction. In general, the results of this calculation show that a more in-depth analysis including all core states is needed before any definitive analysis of the magnitude of error resulting from using the muffin-tin type crystal potential can be made, and that particular attention should be paid to the core orthogonalization. The 4s and 4p states should also be included in the Bloch sums to give a more complete picture of the band structure of copper. Noticing the small number of the basis functions expressed in GTO's used in the final trial wave function, and the results thus obtained in this calculation, which are at least comparable to those reported by using other methods, one feels justified to conclude that the extended tight-

binding approach with non-muffin tin potential and GTO basis constitutes an efficient method to treat the band structures for transition metals.

BIBLIOGRAPHY

- (1) Krutter, H. M., Phys. Rev., 48, 664 (1935).
- (2) Howarth, D. J., Proc. Roy. Soc. (London) A220, 513 (1953).
- (3) Fong, C. Y. and M. L. Cohen, Phys. Rev. Letters, 24, 306 (1970).
- (4) Fukuchi, M., Progr. Theoret. Phys. (Kyoto) 16, 222 (1956).
- (5) Burdick, G. A., Phys. Rev., 129, 128 (1963).
- (6) Snow, E. C. and J. T. Waher, Phys. Rev., 157, 570 (1967).
- (7) Howarth, D. J., Phys. Rev., 99, 469 (1955).
- (8) Segall, B., Phys. Rev., 125, 109 (1962).
- (9) Bulter, F. A., F. K. Bloom, Jr., and E. Brown, Phys. Rev., 180, 744 (1969).
- (10) Loucks, E., Augmented Plane Wave Method, W. A. Benjamin, Inc., New York (1967).
- (11) Herman, F., Rev. Mod. Phys. 30, 102 (1958).
- (12) Pincherle, L., Reports on the Progress of Physics, 23, 367 (1960).
- (13) Slater, J. C. and G. F. Koster, Phys. Rev., 94, 1498 (1954).
- (14) Lafon, E. E., and C. C. Lin, Phys. Rev., 152, 579 (1966).
- (15) Tyler, J. M., T. E. Norwood and J. L. Fry, Phys. Rev. B1, 297 (1970).
- (16) Tyler, J. M. and J. L. Fry, Phys. Rev. B1, 4604 (1970).
- (17) Norwood, T. E. and J. L. Fry, Phys. Rev. B2, 472 (1970).
- (18) Callaway, J. and J. L. Fry, "Towards Self-Consistency With Tight-Binding Approximation", in Computational Methods in Band Theory edited by Marcus, P. M., J. F. Janak, and A. R. Williams, Plenum Press, New York (1971), p. 512.
- (19) Clementi, E., Tables of Atomic Functions, San Jose Laboratory, IBM, San Jose, California (1965).

- (20) Slater, J. C., *Phys. Rev.*, 81, 385 (1951).
- (21) Tinkham, M., Group Theory and Quantum Mechanics, McGraw-Hill Book Company, Inc., New York (1964), p. 32.
- (22) Hamermesh, M., Group Theory, Addison-Wesley Publishing Company, Inc., Reading, Mass. (1962), p. 86.
- (23) Koster, G. F., J. D. Dimrock, R. G. Wheeler, and H. Statz, Properties of the Thirty-Two Point Groups, M.I.T. Press, Cambridge, Mass., (1963).
- (24) Mattheiss, L. F., *Phys. Rev.*, 134, A970 (1964).
- (25) Kotani, M., A. Amemiya, E. Ishiguro, and T. Kimura, Tables of Molecular Integrals, Maruzen Co., Ltd., Tokyo, Japan (1963).
- (26) Shavitt, I., in Methods in Computational Physics, edited by Adler, B., S. Fernbach, and M. Rotenberg, Academic Press Inc., New York (1963), Vol. 2, p. 1.
- (27) Barnett, M. P., in Methods in Computational Physics, edited by Adler, B., S. Fernbach, and M. Rotenberg, Academic Press Inc., New York (1963), Vol. 2, p. 95.
- (28) Snow, E. C., *Phys. Rev.*, 171, 785 (1968).
- (29) Berglund, C. W, and W. E. Spicer, *Phys. Rev.* 136, A1D44 (1964).
- (30) Fadley, C. S. and D. A. Shirley, *Phys. Rev. Letters*, 21, 980 (1968).
- (31) Callaway, J., Energy Band Theory, Academic Press, Inc., New York, (1964), p. 191.
- (32) Howarth, D. J., *Phys. Rev.*, 99, 469 (1955).
- (33) Conolly, J. W. D., *Phys. Rev.*, 159, 415 (1967).
- (34) Slater, J. C. in Methods in Computational Physics, edited by Adler, B., S. Fernbach, and M. Rotenberg, Academic Press, Inc., New York (1968), Vol. 8, p. 1.

VITA²

Lin Wang

Candidate for the Degree of

Doctor of Philosophy

Thesis: ELECTRONIC ENERGY BAND STRUCTURE OF COPPER BY TIGHT-BINDING METHOD

Major Field: Physics

Biographical:

Personal Data: Born in Antung, Manchuria, China, June 11, 1929, the son of Lu-Ting and Shou-Jean Wang.

Education: Attended the Second High School of the City of Antung, and graduated from the Preparatory School of the National Northeastern University, Mukden, Manchuria, China; received the B.S. degree from the National Taiwan University, Taipei, Taiwan, in 1956; received the M.S. degree from Oklahoma State University, Stillwater, Oklahoma in 1966.

Organization: Member of American Physical Society, American Association of Physics Teachers, and Sigma Xi National Science Society.